Theses and Dissertations

Summer 2013

Development of a novel balance assessment tool and its validation in the study of patients with symptomatic spinal deformity

Monica Paliwal
University of Iowa

Recommended Citation

Paliwal, Monica. "Development of a novel balance assessment tool and its validation in the study of patients with symptomatic spinal deformity." MS (Master of Science) thesis, University of Iowa, 2013.
http://ir.uiowa.edu/etd/4891.

www.manaraa.com

DEVELOPMENT OF A NOVEL BALANCE ASSESSMENT TOOL AND ITS

VALIDATION IN THE STUDY OF PATIENTS WITH SYMPTOMATIC SPINAL

DEFORMITY

by

Monica Paliwal

A thesis submitted in partial fulfillment
of the requirements for the Master of Science degree in
Biomedical Engineering in the Graduate College of
The University of Iowa

August 2013

Thesis Supervisors: Associate Professor Sergio Mendoza
Professor Nicole Grosland

Graduate College
The University of Iowa
Iowa City, Iowa

CERTIFICATE OF APPROVAL

_____

MASTER'S THESIS

_____

This is to certify that the Master's thesis of

Monica Paliwal

has been approved by the Examining Committee for the thesis requirement for the Master
of Science degree in Biomedical Engineering at the August 2013 graduation.

Thesis Committee: _____
                    Sergio Mendoza, Thesis Supervisor

                  _____
                    Nicole Grosland, Thesis Supervisor

                  _____
                    David Wilder

                  _____
                    Laura Frey Law

                  _____
                    Tae-Hong Lim

To my parents and my brother

ACKNOWLEDGEMENTS

I would like to take this opportunity to thank everyone who assisted me throughout the development and execution of this project.

I am thankful to Dr. Sergio Mendoza for being my advisor. His constant motivation and guidance has helped me enhance my knowledge and understanding.

I would like to acknowledge Dr. Christopher Graves for his assistance in the development of the data acquisition software. I appreciate the help of Ms. Rachel Nash in recruiting subjects for this study.

I would like to thank Dr. David Wilder for his guidance in the development of the point loading device. I am thankful to Dr. Laura Frey Law for her invaluable input in the calibration procedure.

I would also like to thank Dr. Nicole Grosland and Dr. Asghar Bhatti for their valuable assistance and guidance in different technical aspects of the project.

Finally, I would like to thank my parents. They have been a constant source of inspiration and encouragement. I am deeply thankful to my friends for their loving support throughout my struggles and their appreciation on my accomplishments.

TABLE OF CONTENTS

v

LIST OF TABLES

LIST OF FIGURES

viii

CHAPTER 1: INTRODUCTION

<u>Statement of the Problem</u>

Postural Stability and Balance

Balance is defined as the ability of human body to maintain center of gravity within the base of support to prevent falling[1]. Maintenance of balance requires coordination between sensorineural and musculoskeletal systems. A number of medical conditions can impair function of any of these systems and thereby predispose individuals to postural instability, loss of balance and falling. Aging, obesity, vestibular deficits, neurologic conditions, abnormal spinal curvatures, peripheral neuropathies etc. are known to affect balance.

There is a high prevalence of falls among the elderly. Falls in older adults are a major cause of death, fractures and traumatic brain injuries that affect quality of life and independent living. Falls resulting from postural instability and impaired balance put considerable economic burden on health care system and is a major public health issue[2]. Obesity changes the mass distribution between body segments and is associated with poor postural control. Higher body mass index (BMI) results in instability in medio-lateral and anterior- posterior directions. Obese older adults have higher prevalence of falls as compared to their normal weight counterparts[3]. Neurologic disorders such as multiple sclerosis[4], parkinson's disease, cerebral palsy etc. are significantly associated with an increased instability and fall risk. Arthritis and injury to lower limbs such as ankle sprains and other orthopedic pathologies are known to contribute to balance problems. Spinal deformities shift the location of center of gravity in anterior-posterior or

medio-lateral directions, thereby challenging the balance system. Therefore, evaluation of postural instability and assessment of balance is of critical value in clinical practice.

Assessment of Balance

A number of balance measurement scales have been developed. Scales based on self-reported questionnaires regarding fall history, activity levels etc., others based on functional evaluation such as Romberg test, Forward reaching test, Timed up and go, Performance oriented Mobility Assessment (POMA), Berg balance etc. are commonly used in clinical practice[5, 6, 7]. These tests are accessible in various clinical settings and economically feasible in terms of time, cost, labor and equipment. Although functional tests are advantageous because of their practicality, simplicity and inexpensive nature, these do not provide information and cannot identify minor changes or damages in balance control system. Only a few scales have been shown to have significant associations with increased fall risks. There is not enough supporting evidence in favor of any specific balance measurement scale in assessing the risk of fall from the outcome score of the scale. Moreover, the results of the balance tests can differ depending upon the diagnostic test used[8].

Force plates are considered gold- standard for assessment of balance. Center of pressure (COP) is the location of the ground reaction force that can be recorded through force plates. It is an accurate and reliable measure of balance and stability. Force plates provide information about the medio-lateral and anterior posterior displacements of COP signal. COP can be used to study the effect of sensorineural and muscular systems in control of balance. Analysis of COP signal can provide insight in the use of different

strategies for maintaining balance. Output parameters such as COP path length and area are direct measures of postural stability.

Despite its advantages, force plate technology is seldom used outside laboratories and research environments because of its expensive instrumentation and operational complexity. Also, the process of operation is time consuming and requires a trained technician for its use and interpretation of results. These factors limit its availability and use by clinicians and therapists.

A Wii Balance Board (WBB) is an accessory to the Nintendo Wii game console. It consists of four pressure transducers and can be programmed to perform as a force plate by capturing COP signal. It is an inexpensive, widely available and portable device. Its validity and reliability in assessment of standing balance against laboratory grade force platforms has been tested in literature[9]. Excellent test-retest reliability and intra - class correlation coefficient has been reported. Hence it can be used as an alternative consumer level force plate[9, 10].

The purpose of this project was to program a WBB to track COP signal using data acquisition software (LabView) and to develop an integrated, graphical user interface (GUI) based system that can be used to assess balance in the clinical setting.

Aims

The study consisted of the following four aims.

1.   Develop user friendly software that functions to capture, process and display COP signal from the WBB.

2.   Develop a calibration protocol and test the performance of WBB in terms of linearity and hysteresis.

3.   Calculate balance parameters: Path Length, Sway Area and Sway Velocities.

4.   Clinical testing of the software: Prospective cohort study, comparing balance parameters between a known balance deficit population- spinal deformity patients vs. age, BMI and sex matched controls.

<u>Balance in Patients with Spinal Deformity</u>

Spinal deformities encompass a variety of conditions that affect the normal spino-pelvic alignment in coronal or sagittal plane or longitudinal axis (rotational deformity). Common presenting symptoms include progressive deformity, pain in back and lower extremities[11].

The center of balance in sagittal plane deformity patients is widely studied radio-graphically using sagittal vertical alignment (SVA). The measurements are performed radio- graphically by dropping a plumb line from Cervical 7 vertebra, and measuring the horizontal distance from the center of the plumb-line to the posterior-superior corner of Sacral 1 vertebra.

A variety of changes in the spine, pelvis and lower extremities are observed in patients to compensate for anterior shift in the gravity line. A few compensatory mechanisms reported in literature are reduction of thoracic kyphosis, hyper-extension of spinal segments, retrolisthesis in spine, pelvic retroversion, and knee flexion and ankle extension in lower limbs[12]. These mechanisms appear progressively to correct increasing imbalance and bring the axis of gravity in physiologic position.

Jean Dubousset, first introduced the concept of 'cone of balance', referring to a stable region of standing posture, deviating outside the cone pose challenges to balance mechanisms[13]. The ability of the human body to maintain the center of gravity (COG) within the cone of economy with minimal energy expenditure results from a complex interaction of supra- and infra-pelvic alignment parameters.

Of many spine and pelvic radiographic alignment parameters, multiple studies show that trunk imbalance correlates with poor quality life outcomes scores and progressively worsening low back pain[14, 15, 16]. Trunk imbalance is measured by the SVA (Sagittal Vertical Alignment). These correlations do not explain symptoms for every case, and there are notable examples of patients with severe deformity and minimal functional loss, as well as others with not-so-severe deformity and severe functional loss[14]. The way individual patients tackle trunk imbalance may be variable and may depend on other constitutional factors such as age, baseline cardiovascular conditioning, and BMI.

The aim of this study is to validate WBB based novel evaluation tool for the study of adult spinal deformity by examining balance parameters in comparison with healthy control population. Changes in postural stability due to presence and severity of sagittal imbalance (SVA) in relation with compensatory mechanism- pelvic retroversion are analyzed.

One of the functions of spine in the body is to transfer loads from upper body to pelvis and lower extremities in order to maintain an upright standing posture. Presence of spino-pelvic misalignment would produce some degree of postural instability. It is hypothesized that although compensatory mechanisms may correct for positive SVA,

assuming these postures puts high energy demands on the musculoskeletal system resulting in fatigue, pain and postural instability.

Patients with low back pain have a demonstrable larger postural sway with smaller thoraco-lumbar movements. This represents a rigid postural control strategy, maybe a protective mechanism, based on the increasing use of ankle balancing strategies[17, 18, 19]. In patients with trunk imbalance, the paraspinal muscles are at increased mechanical demand, and may thus mimic the rigid postural control strategies described for low back pain patients. Similarly, this would also reflect in increased postural sway.

Specific Hypotheses

H1 = Path length, sway velocity and sway area will be higher for patients than in controls.

It has been theorized that mechanisms to compensate for anatomical sagittal plane imbalance in patients result in postures that put high musculoskeletal loads and demand high-energy expenditure to maintain these postures, consequently fatiguing the musculature and aggravating pain.

H2 = Path length, sway velocity and sway area will increase in groups with progressive sagittal imbalance and presence of compensatory mechanisms.

CHAPTER 2: LITERATURE REVIEW

Postural Instability

Maintenance of an erect posture during quiet standing requires a continuously acting control mechanism to prevent from falling. Human balance control during quiet standing has been described as an inverted pendulum about the ankle joint[1]. Maintenance of balance depends on proprioception through sensory and motor systems; postural control requires the coordination between musculoskeletal elements of the body.

A number of pathologies are known to affect the balance system. Various studies have reported that aging, neurologic disorders, obesity, lower limb osteoarthritis, injury, abnormal spinal curvatures etc. can result in significant postural instability.

Aging is associated with poor neuromuscular control and high prevalence of osteoarthritis[10]. Falls in the elderly is a public health issue. In 2010, direct medical costs of falls were estimated to be $30.0 billion. Falls in older adults are a major cause of death, fractures and traumatic brain injuries that affect quality of life and independent living[20]. Prevalence of obesity is growing rapidly. In 2009-2010, CDC reported that more than one-third of the US adults are obese[21]. Obesity is associated with poor postural control. Higher body mass index (BMI) have been shown to result in instability in medio-lateral and anterior- posterior directions[22, 23]. Obese older adults have higher prevalence of falls (27% vs. 15%) as compared to their normal weight counterparts[3]. Neurologic disorders such as multiple sclerosis[4], parkinson's disease, cerebral palsy are significantly associated with an increased instability and fall risk. Spinal deformities shift the position of center of gravity in anterior-posterior or medio-lateral directions, thereby challenge

balance system[24]. Since, balance is affected as a result of numerous disease processes of such wide-spread occurrence, evaluation of postural instability and assessment of balance is important.

Balance Assessment Scales

Balance assessment scales developed and widely used in clinics and rehabilitation centers are often based on functional performance of the individuals. Few of the widely used scales that are found are the Berg Balance Scale (Berg), the Clinical Test of Sensory Interaction and Balance (CTSIB), the Functional Reach Test, the Tinetti Balance Test of the Performance-Oriented Assessment of Mobility Problems (Tinetti), the Timed "Up and Go" Test (TU&GT), Physical Performance Test (PPT), tandem stand, tandem walk, one legged stance etc.

Functional tests require the subject to perform a few day to day tasks and assign a score to the task depending on the time taken to perform the task or the level of difficulty experienced. These tests are usually easy to run, cost effective, time efficient, and do not require much instruments. These can be administered in mostly any clinical setting by any therapist. Due to these reasons, functional assessment tests are widely used.

However, these tests have a number of limitations. These tests are highly subjective, often depending on self-reported values. The validity and reliability, sensitivity and specificity of the tests are variable. There can be variability in the test result depending upon the selection of the diagnostic test and selected cutpoints. Only a few scales such as tandem stand, tandem walk, one legged stance etc. have been shown to have significant correlation with fall risk. No one scale has been identified to be better over others in quantifying balance and assessing fall risks[8]. These tests do no provide

information about force distribution, which underlying system involved in balance control is damaged or which muscle groups are involved in maintenance of balance.

Force Plate technology and Wii Balance Board

Generally, commercially available, laboratory grade force plates are recognized as an outstanding tool for assessing balance due to their ability to accurately measure COP. COP signal gives the point location of the ground reaction force. Force plates provide the COP displacement or excursion in anterior-posterior and medio-lateral directions. COP signal is the only major measure of balance that gives the information about the center and maintenance of balance from the biomechanical point of view. During quiet standing, in order to assume a steady posture, the COP should lie within the base of support, (i.e. the perimeter of the feet). Control of COP signal in the anterior- posterior direction is by ankle muscles while the medio-lateral control requires activation of the hip muscles. The COP excursions, as provided by the force plates, can be analyzed to provide information about activity of different muscle groups. The signal can be processed to provide output measures of balance such as path length, sway velocity and area to provide detailed picture of instability. Researchers in the past have also used the frequency domain analysis of the COP signal to study balance[25].

However, there are limitations to the use of such force plates outside research environments. High cost, non-portability, custom setup and training required for its operation hinder its widespread use.

The WBB has been recognized as a tool that can be programmed to mimic the function of force plate based technology by capturing the COP signal[9, 10]. It has been shown to have excellent accuracy and reliability when compared with traditional force

plates to determine center of pressure in balance studies[9, 10]. The device is widely available, costs less than \$100, is not bulky and thus is portable. Clark et al.[9] studied the performance of the WBB against a lab-grade Kistler force plate. The study recruited thirty healthy individuals without any lower limb pathology. The subjects were asked to stand on the WBB and force plate in four different conditions: (1) single leg, (2) double leg, (3) eyes open and (4) eyes closed. The output measure, path length was defined as the total distance travelled by the COP signal. The WBB was shown to produce good test –retest reliability for COP path length as studied by within device intraclass correlation coefficients (ICC = 0.77–0.89). The study concluded that a WBB is a valid tool for the study of standing balance and can be used as a consumer level alternative to the force plate.

Historically, study of balance in spinal deformity patients has been done via use of radiography. Sagittal plane deformity, compensatory mechanisms for the correction of imbalance, study of balance using radiographic parameters and its limitations underscoring the need to study balance using COP are introduced in the following section.

<u>Spinal deformities and Sagittal Imbalance</u>

The prevalence of spinal deformity in individuals over the age of 60 years varies between 39%[26, 27] and 68%[26, 28]. Spinal deformities encompass a variety of conditions that alter normal anatomical alignment of spine in 3D, i.e. coronal or sagittal plane such as scoliosis, kyphosis, spondylolisthesis, iatrogenic flat back etc. Adult idiopathic scoliosis may be caused by arthritis and process of aging, however cases of congenital and

adolescent scoliosis are also found. Common presenting symptoms include progressive deformity, pain in back and lower extremities.

Sagittal vertical alignment (SVA) is widely used to study sagittal plane deformities. It is accepted as an important and reliable predictor of health status in the adults with spinal deformity[14]. It is measured radio- graphically by dropping a plumb line from the center of C7 vertebra, and measuring the horizontal distance from the center of the plumb-line to the posterior corner of S1 endplate[28]. Figure 1 shows SVA measurement in a balanced and an imbalanced spine. Note that the imbalanced spine is marked by positive SVA. Glassman[14, 15] found a significant correlation between positive SVA and decreased quality of life in patients with symptomatic spinal deformity.

<div align="center">Compensatory Mechanisms</div>

Sagittal plane deformities resulting in positive sagittal imbalance hinder in assuming an erect standing posture. A variety of changes in the spine, pelvis and lower extremities are observed in patients to compensate for anterior shift in gravity line. A few compensatory mechanisms reported in literature are reduction of thoracic kyphosis, by hyper-extension of spinal segments proximal to the spinal deformity, retrolisthesis in spine, hip extension, and knee flexion and ankle extension[30]. These mechanisms appear progressively to correct increasing imbalance and bring the axis of gravity in physiologic position[31]. Figure 2 shows the various compensatory mechanisms at the spine, pelvic or lower limb level that may be present in patients with positive sagittal imbalance.

Pelvic retroversion is the backward tilt of the pelvis over the femoral heads. It is the first mechanism to set in to correct for sagittal imbalance[31]. Figure 3 a shows a severely imbalanced spine with positive SVA; Figure 3 b shows the use of pelvic

retroversion to correct imbalance. Pelvic tilt (PT) is defined as the angle subtended by the vertical axis originating from the center of the femoral head and the midpoint of the sacral endplate. It is a positional parameter that measures the compensation by pelvic rotation[32].

Cone of Balance

Jean Dubousset first introduced the concept of 'cone of balance', referring to a stable region of standing posture, where the energy expenditure for stance is minimized. Deviations from this cone pose challenges to balance mechanisms[13]. Figure 4 illustrates the 'cone of balance'.

In humans, two-thirds of the body mass is located at two-thirds height above the ground. The ability of the human body to maintain the center of gravity (COG) within the cone of economy with minimal energy expenditure results from a complex interaction of supra- and infra-pelvic alignment parameters. These parameters are influenced by the flexibility of the spine and joints of the lower extremities, neuro-muscular control, strength, endurance, and body habitus. It becomes evident that the impact of spinal deformity on stance is multi-factorial, and thus cannot be exclusively correlated to static alignment parameters. Thus center of pressure measurements become particularly relevant in the study of the factors that influence or determine symptoms in patients with spinal deformity.

Arm Position for Lateral Radiograph Acquisition

In normal stance, we usually place our hands on the sides of our thighs. Acquisition of lateral radiographic images for study of the spine requires clearing of the humerus from the proximal thoracic spine for visualization purposes. Arms crossed on

chest, elbows flexed at various angles, arms supported on the wall, fists on clavicle etc. are commonly used positions in different institutions. A number of studies aimed at evaluating the effect of arm position on thoracolumbar spinal alignment and SVA, attempting to identify an optimal, functional arm position are found in literature. Results of these studies indicated that some positions may be better than others in terms of variance in SVA readings; however none of the positions represented a functional standing position [34, 35, 36, 37]. Radiography is affected by positioning protocol and thus not a reliable in evaluating sagittal profile and balance.

In addition to this, radiography has a degree of inter-observer and intra-observer variance, represents spino-pelvic alignment only a single frame of time and does not offer information on foot position or force distribution.

Although spine-pelvic parameters obtained by radiographic measurements are widely used in practice, optimal way to study global balance is using force plates and assessing center of pressure (COP). There is controversy over the accuracy of radiographic measurements in representing true center of balance as compared to COP on force plates[38, 39].
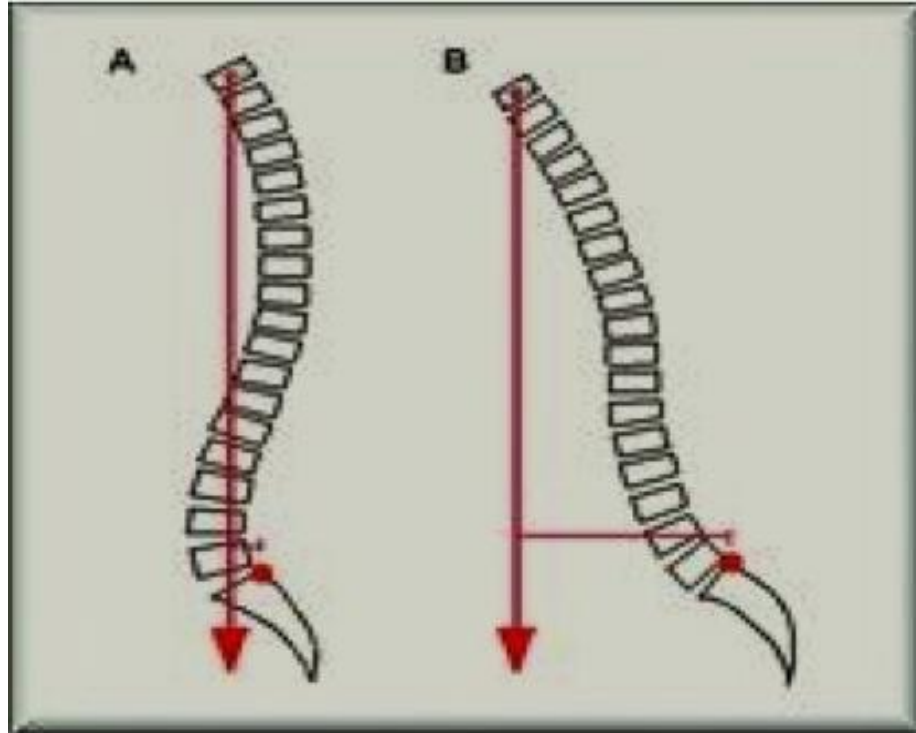
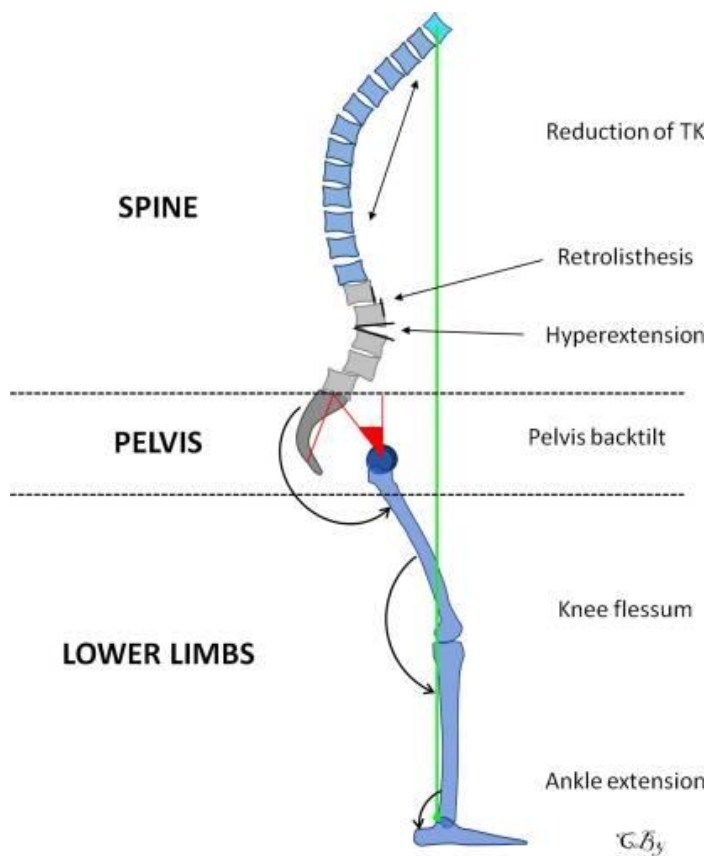Figure 1. Sagittal balance- A. Balanced B. Imbalanced

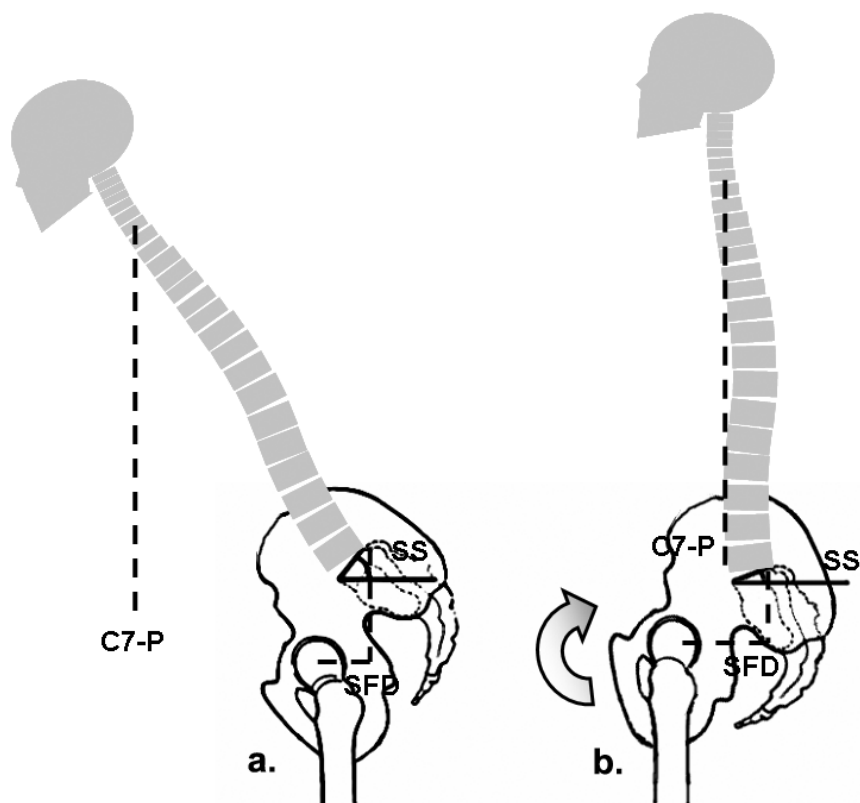Figure 2. Compensatory mechanisms [Source- C Barrey et al. 2011][30]

Figure 3. Pelvic retroversion [Source- Mendoza-Lattes S. et al 2010][33]
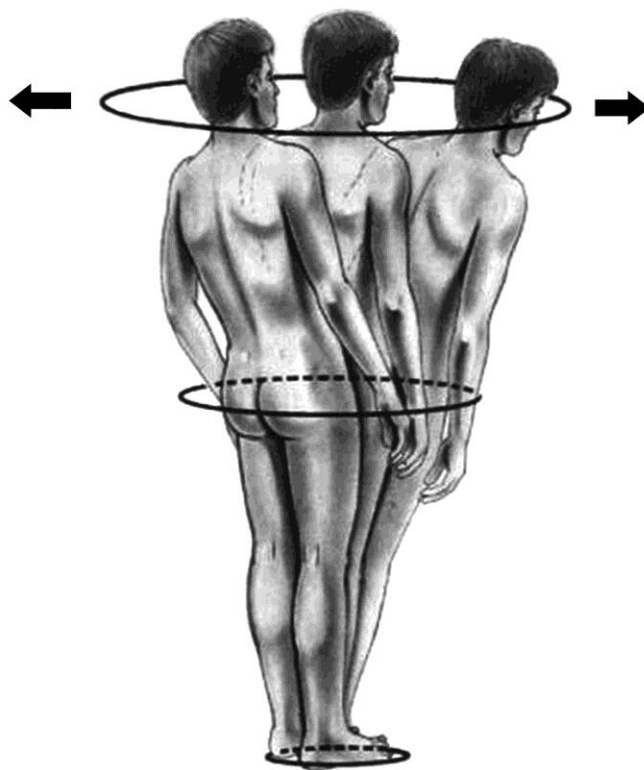
Figure 4. Cone of balance [Source- Dubousset J 1994][13]

CHAPTER 3: MATERIALS AND METHODS

Data Acquisition

A WBB has four strain gauge type transducers at each corner that detect and convert force into electrical signal. The WBB has inbuilt circuitry consisting of an analog to digital convertor and a BCM2045 chip for Bluetooth connection with any computer. Custom data acquisition software had been developed using a standard software toolkit (LabView) to capture the force outputs from each sensor and is available as open source[40].

Building upon the open source code, additional software was written to calculate vertical ground reaction force and location of the COP coordinates (X, Y) using the following equations.

$$Fz = F_{TL} + F_{BL} + F_{BR} + F_{TR}$$

$$X = F_{TR} + F_{BR} - F_{BL} - F_{TL}$$

$$Y = F_{TR} + F_{TL} - F_{BL} - F_{BR}$$

Where- Fz: Total ground reaction force, F_{TL}: Force from Top-Left sensor, F_{BL}: Force from Bottom-Left sensor, F_{TR}: Force from Top-Right sensor, F_{BR} : Force from Bottom-Right sensor.

Note that the coordinates of the COP (X, Y) were recorded in terms of forces. However, the calibration of location of COP(X, Y) was performed later to derive X, Y in units of distances.

A Graphical user interface as shown in Figure 5, was designed comprising of features such as display of COP signal in real time, specification of data recording time,

and routines for saving the data. Data was saved in Excel format and exported to MatLab for signal processing and analysis.

Calibration

Point Loading Device

The process of calibration requires point loading on the surface of the WBB. Few point loading mechanisms developed for this purpose can be found in the literature. Bobbert and Schamhardt[41] used a sturdy wooden board supported on a ball stylus at one corner for point loading. Weights were loaded on the wooden board while the board was kept level by supporting other corners outside the periphery of force plate. Collins et al. employed an instrumented pole for calibrating force plates. The pole had a loading plate at one end to put weights, conical tip at the base to ensure axial loading. Motion tracking markers and a load cell were applied to the pole to monitor the 3D orientation of the pole and axial force respectively[42].

In this project, to calibrate WBB, a point loading device was designed. The working principle is that the center of gravity of an equilateral triangle passes through its centroid. The device consists of an annular disc supported on three conical stainless steel pegs, with a hollow vertical pole to slide down disc weights and acrylic see-through glass with a cross-wire in the middle. [D.G. Wilder, personal communication, 2012]. Figure 6 shows the point loading calibration device.

Consequently, the three pegs established the vertices of an equilateral triangle with its centroid coinciding with the center of the cross-wire. Disc weights can be aligned on top of one another during loading by sliding them down the vertical pole. The weights

rest on annular disc, which is in turn supported by the pegs. The support reaction from the ground will be equally distributed among the three pegs.

The tips of the conical pegs were rounded to 1mm in radius, to avoid digging or scratching of the WBB surface.

Calibration Procedure

Data acquisition software was programmed to report forces from all force sensors (top-right TR, top-left TL, bottom-right BR and bottom-left BL), ground reaction force and COP displacement in medio-lateral (X) and anterior-posterior (Y) directions. Calibration of the WBB was a two-step process involving (1) calibration of the ground reaction force and (2) calibration of the location of COP (X, Y).

I.   Calibration of Ground Reaction Force

Protocol:

The following steps were performed on all corners of the board, at each sensor individually:

1. A full cycle of loading and unloading of point loads of 12N, 34N, 56N, 78N, 101N, 123N, 167N, 212N, 256N were applied on the sensor (Figure. 9).

2. Data was collected for three seconds. Forces from each sensor F_{TR}, F_{TL}, F_{BR} and F_{BL} were recorded for each trial. Total ground reaction force F_Z was calculated as:

    $F_Z = F_{TR} + F_{TL} + F_{BR} + F_{BL}$

3. Linearity of each sensor was studied by regression analysis between applied load and recorded sensor force.

4. Calibration factor C, defined as the slope of known versus recorded forces was calculated as $= \frac{Applied\ force}{Measured\ Force}$.

5. Percent full scale output (%FSO) hysteresis error (*% e (h)*) was calculated for each cycle of loading, expressed as:

$$\% \, e(h) = \frac{\max(|y_{up} - y_{down}|)}{y_{max} - y_{min}} * 100$$

Where y_{up} – output during upscale loading, y_{down} – output during downscale loading, y_{max} – maximum output, y_{min} – minimum output.

The maximum error of the four cycles was reported.

6. %FSO linearity error (*% e (l)*) was calculated for each cycle of loading as:

$$\% \, e(l) = \frac{\max(|y_{L} - y_{true}|)}{y_{max} - y_{min}} * 100$$

Where y_{L} – Best linear regression output, y_{true} – True output, y_{max} – maximum output, y_{min} – minimum output.

The maximum error of the four cycles was reported.

Figure 7 shows the loading of the weights on the WBB sensor for the calibration of ground reaction force.

II. Calibration Of Center of Pressure Location

The coordinates of COP (X, Y) on a force plate according to Kistler[43] is given by the following equations:

$$X = \frac{Z * F_x + [(F_{BR} + F_{TR} - F_{BL} - F_{TL}) * CalX]}{Fz}$$

$$Y = \frac{Z * F_y + [(F_{TR} + F_{TL} - F_{BL} - F_{BR}) * CalY]}{Fz}$$

Where, Z = vertical distance between working plane and X, Y plane of force platform,

F_x = Total force in X direction, F_y = Total force in Y direction,

F_Z: Total vertical force, F_{TL}: Force from top-left sensor, F_{BL}: Force from bottom-left sensor,

F_{TR}: Force from top-right sensor, F_{BR}: Force from bottom-right sensor,

CalX = half the distance between the sensors along the X axis

CalY = half the distance between the sensors along the Y axis.

The WBB sensors cannot detect forces in the horizontal directions (F_x and F_y), hence adjustments in the COP (X, Y) calculations were made to account for lack of sensitivity in WBB to shear forces.

The following procedure was performed to accurately determine the values of *CalX* and *CalY* for the WBB.

A grid of 2cm by 2cm was plotted on the surface of the WBB. Sixteen different points, four points in each quadrant on the WBB were selected as trial points. Loads of 12N, 34N, 56N, 78N, 101N, 123N, 167N, 212N, 256N were applied on each trial point. A total of 144 trials were performed. Forces from each sensor, total ground reaction force, COP(X) and COP(Y) locations data were recorded for 3 seconds. Figure 8 shows the point loading device placed at X= -2cm, Y=2cm point on the 2cm by 2cm grid plotted on the surface of the WBB.

Due to the rectangular geometry of the board, the medio-lateral (X) axis of the board is longer than the anterior-posterior (Y) axis. Hence, *CalX* and *CalY* were calculated separately as given below:

$$CalX = \frac{Known\ X}{\dfrac{Recorded\ X}{Fz\ (Uncalibrated)}} \ , \quad CalY = \frac{Known\ Y}{\dfrac{Recorded\ Y}{Fz\ (Uncalibrated)}}$$

The calibrated values of *X (Xc)* and *Y (Yc)* are given as:

$$Xc = \frac{(F_{BR} + F_{TR} - F_{BL} - F_{TL}) * CalX}{Fz \ (calibrated)}$$

$$Yc = \frac{(F_{TR} + F_{TL} - F_{BL} - F_{BR}) * CalY}{Fz \ (calibrated)}$$

Where,

$Recorded \ X = F_{TR} + F_{BR} - F_{BL} - F_{TL}$ and $Recorded \ Y = F_{TR} + F_{TL} - F_{BL} - F_{BR}$

Correlation plots between *Known X* vs. *Xc* and *Known Y* vs. *Yc* were produced. Average percentage error between *Known* and *calibrated* values of COP(X, Y) was calculated as:

$$\% \ e = \frac{|calibrated \ value - known \ value|}{|known \ value|} * 100$$

Signal Processing and Output Parameters

Custom software was written in MatLab for signal processing and calculation of output parameters. COP data was imported and power spectral analysis using Fast Fourier Transform (FFT) was done to find noise frequency component in the signals. Figure 9 shows the power spectral density of the COP signal. The peak in the graph corresponds to the frequency of the COP signal. The cut-off frequency for the low pass filter was chosen to be 5Hz to filter out higher frequency noise.

A zero-phase lag, eighth order low pass Butterworth filter with a cut-off frequency of 5Hz was designed to filter the data.

Ideally, the sampling rate of data collection by the WBB is 60 Hz. However, due to various reasons such as poor quality of the sensors, weak blue-tooth connection the number of samples collected per second may vary. The average sampling rate of the WBB used in this study was found to be 54 Hz. The data were then down sampled to 45 Hz using signal processing in MatLab. Figure 10 shows a 30 second long raw COP data,

filtered data and down sampled data versus time frames. Note that the numbers of frames were reduced to 1330 from 1620 when the signal was down-sampled to 45 Hz from 54Hz.

Following output parameters were calculated:

1. Path length[44]– Path length is the total vector distance travelled by the center of pressure during a trial.

$$PL = \sum \sqrt{(x[n] - x[n+1])^2 + (y[n] - y[n+1])^2}$$

The path length in X and Path length in Y were also calculated to provide information on the direction of major sway (medio-lateral or anterior-posterior).

$$PL(x) = \sum |x[n+1] - x[n]| \qquad PL(y) = \sum |y[n+1] - y[n]|$$

2. Sway area (95% confidence region) [44] – It measures the area of the ellipse formed by 95% of the X, Y coordinates around their mean values during a specified time unit. It is given as:

$$Sway\ Area(CE) = \pi ab = 2 * F_{0.05[2,n-2]} * \sqrt{(s_{xx}^2 s_{yy}^2 - s_{xy}^2)}$$

where - s_{xx} and s_{yy} - standard deviations in x and y, s_{xy}- Covariance between x and y, $F_{0.05[2,n-2]}= 3$; n > 120.

3. Root Mean Square Velocity in X and Y and total RMS velocity.

$$V_{xRMS} = \frac{\sum_{i=1}^{n} vx[n]^2}{n}$$

$$V_{yRMS} = \frac{\sum_{i=1}^{n} vy[n]^2}{n}$$

$$V_{TRMS} = \sqrt{(V_{xRMS}^2 + V_{yRMS}^2)}$$

<u>Clinical Study</u>

Subjects

Ninety –seven patients with spinal deformities (namely, adult idiopathic scoliosis, kyphosis, spondylolithesis and iatrogenic flat back) were recruited from the Orthopaedic Spine Clinic. Patients were subdivided into four groups based on their sagittal imbalance (SVA) and Pelvic Tilt (PT) [32]. Thirty healthy age and gender matched volunteers were recruited. Individuals with history of scoliosis, major spine or lower limb injuries or surgeries, diabetes, strokes, polio, neuromuscular or neurological diseases were excluded from the study. Control subjects were included only if they reported to be able to walk at-least 5 blocks unassisted.

The following table lists the subject groups, number of subjects in each group and mean age and BMI:

S.N.	Subject Groups	Number of subjects (female, male)	Age (years) Mean ± S.D.	BMI ($\frac{kg}{m^2}$) Mean ± S.D.
1	Low SVA (<5 cm), Low PT (<25°)	18 (17 females, 1 male)	52±19	26.1±4.3
2	Low SVA (<5 cm), High PT (>25°)	26 (22 females, 4 males)	58±16	26.8±5.0
3	High SVA (>5 cm), Low PT(<25°)	19 (16 females, 3 males)	62±10	30.9±6.9
4	High SVA (>5 cm), High PT (>25°)	34 (27 females, 7 males)	65±10	30.3±7.0
5	Controls	30 (24 females, 6 males)	55±10	28.6±5.4

Table 1. Subject groups

Demographic data such as weight, height, age and gender were recorded.

Standing radiographs in the sagittal plane were collected on the day of data collection. Radiographic parameters: SVA, defined as the distance between a plumb-line dropped from the center of the C7 vertebra and the posterior border of the sacral endplate was measured. PT, defined as the angle subtended by the vertical axis originating from the center of the femoral head and the midpoint of the sacral endplate was also measured. Subjects were asked to stand on a graph paper with their feet parallel and comfortable distance, usually shoulder's width apart. Distance between the heels and distance between toe and heel were recorded. The WBB was placed six inches in front of a wall. Half the heel-heel distance was marked on the X axis, and half the toe to heel distance was marked on the Y axis of the board. Symmetric placement of feet about the medio-lateral and anterior-posterior axes of the board was assured. Figure 11 shows the positioning of a subject's feet on the WBB.

Trials

Subjects were positioned on the board and asked to keep their knees locked in extension, while resting their arms on the sides (Neutral position) as illustrated in the Figure 12. COP displacement data in medio-lateral and anterior- posterior directions were recorded for 30 seconds.

Analysis

The data was filtered through an 8th order low pass Butterworth filter at a cut off frequency of 5 Hz and down-sampled to 45 Hz.

The COP path length, RMS sway velocity (medio-lateral [X] and anterior-posterior [Y]), RMS Total sway velocity and 95% confidence ellipse area were calculated.

Statistical Analysis

A one-way ANOVA was performed to assess the differences mean path length, sway velocity and 95% sway area between the controls and the four patient groups at a significance level of 0.05.
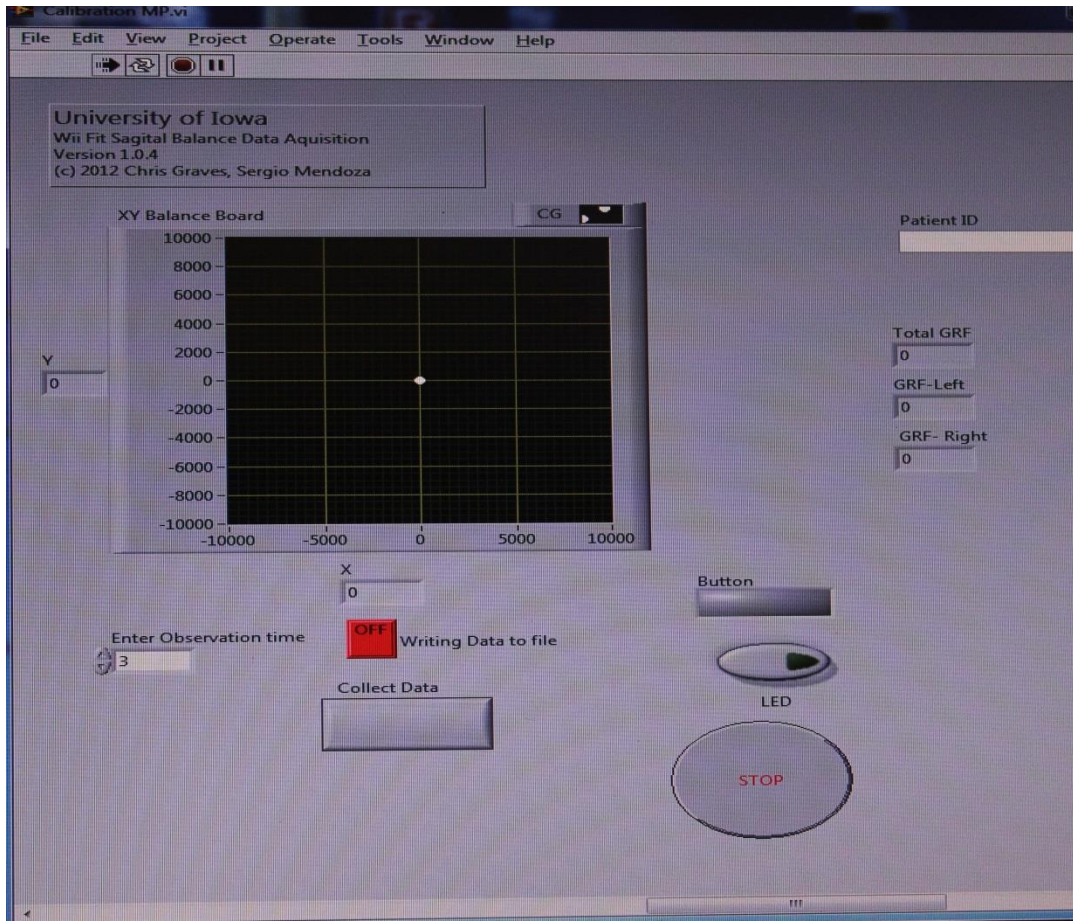
Figure 5. Screen shot of custom graphic user interface (GUI)

Figure 6. Point loading calibration device

Figure 7. Calibration of ground reaction force
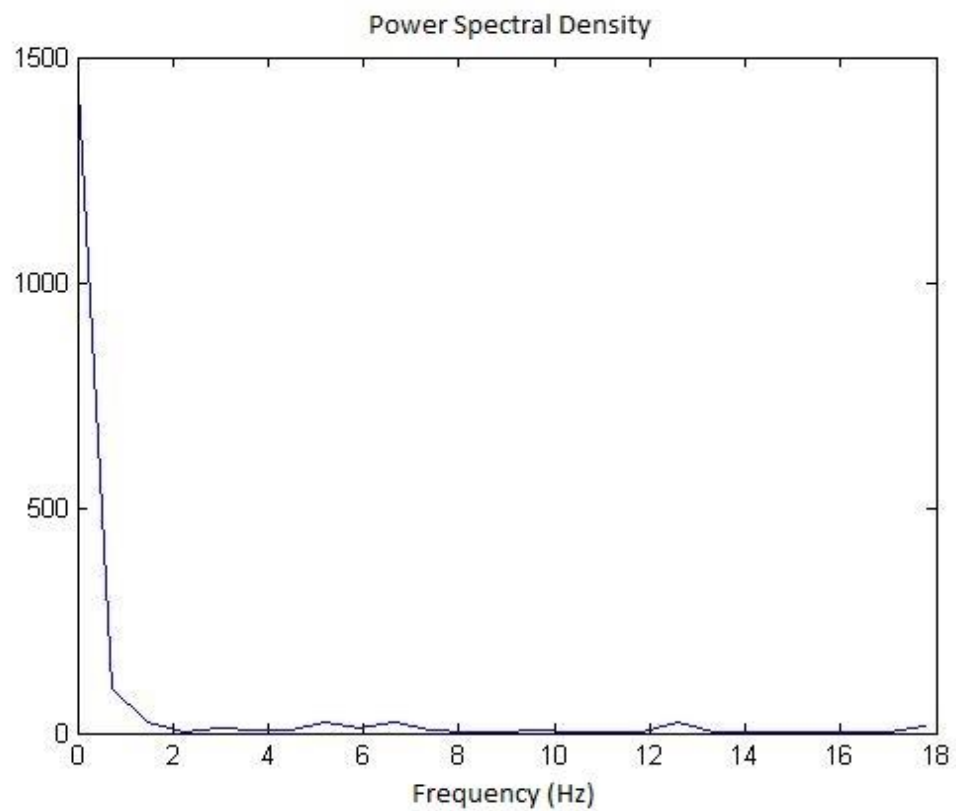
Figure 8. COP (X,Y) calibration set up

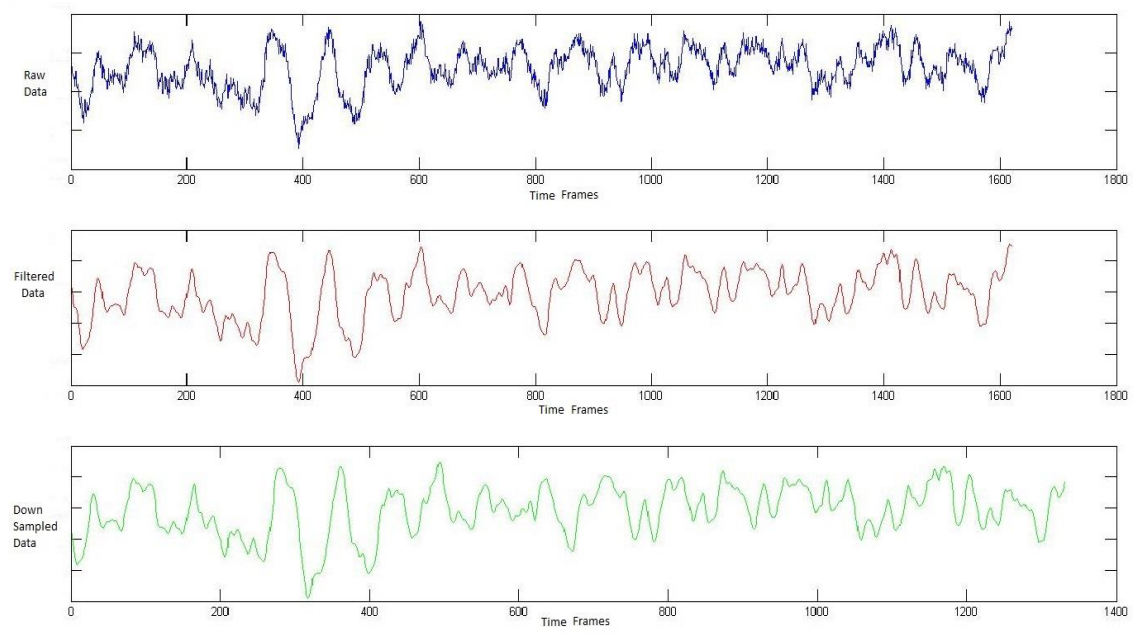Figure 9. Power spectral density of the COP signal

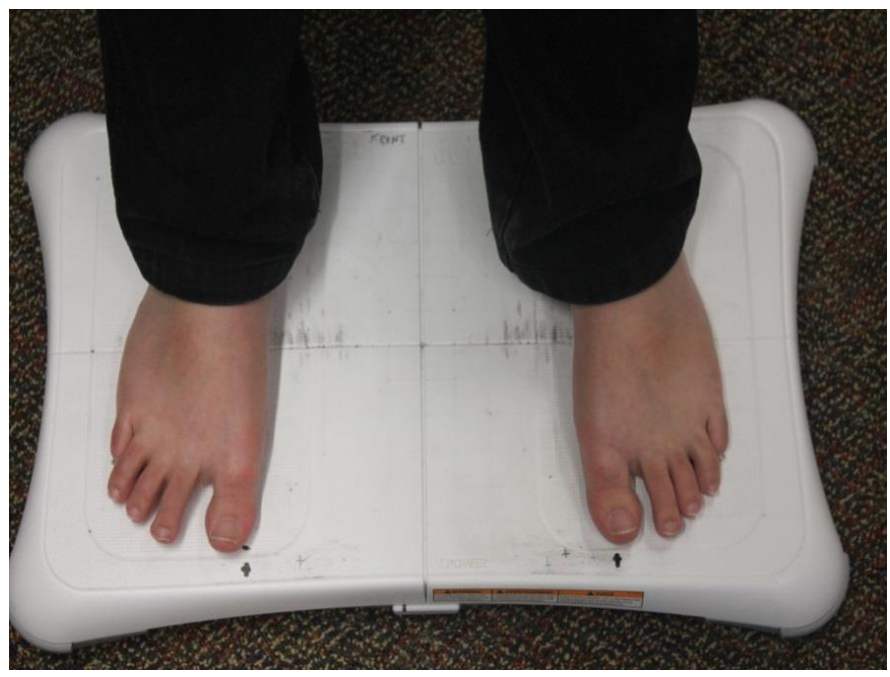Figure 10. Raw data, filtered data and down- sampled data

Figure 11. Feet positioning on the WBB

Figure 12. Standing position- hands on sides (30 sec)

CHAPTER 4: RESULTS

<u>Calibration</u>

Regression analysis between applied force and recorded force from each sensor showed that with increasing magnitude of applied force, there was a linear increase in force detected by the sensor. Figure 13 shows linear correlation between the bottom-left sensor force F_{BL} versus the applied force. $R^2 = 0.999$ was found. Figure 14 shows linear correlation between the bottom-right sensor force F_{BR} versus the applied force. Linear regression equation revealed $R^2 = 0.999$. Figure 15 shows linear correlation between the top-left sensor force F_{TL} versus the applied force. $R^2 = 0.999$ was found. Figure 16 shows linear correlation between the top-right sensor force F_{TR} versus the applied force. $R^2 = 0.999$ was found.

Linearity error in %FSO was calculated for each full cycle performed on four sensors. Maximum of the four cycles was calculated and was found to be <1.75 %FSO. That is the maximum percentage error due to presence of non-linearity in the measurement. Figure 17 shows the applied versus total output force. The best linear curve fit equation was found to be *y=0.9869x+0.0686*. The slope of the line (0.9869) was close to one and thus represents linear operation of the WBB.

Hysteresis error in % FSO was calculated for each full cycle performed on four sensors. Maximum of the four cycles was calculated and was found to be <1%FSO. This is the maximum percentage of error due to difference between upscale and downscale sequential loading. Figure 18 illustrates the hysteresis curve for one full cycle of loading.

Figure 19 represents the calibration curve giving the relation between the measured and calibrated value of the force.

Calibration factor C, defined as the slope of known versus measured force was found to be 0.021893039.

Calibration equation was given by:

$$y = 0.0219x + 0.0155$$

Where, x = measured force in arbitrary units and y = calibrated value of force in lbs.

The value of *Cal X* was found to be 21.48547. It was defined as half the distance between the sensors in X direction and thus represents the distance between the defined origin (0,0) and the sensors in X direction. Similarly, the value of *Cal Y* was found to be 12.21421. It was defined as half the distance between the sensors in Y direction and thus represents the distance between the defined origin (0,0) and the sensors in Y direction.

Figure 20 shows the graph between the *Known X* vs. calibrated value of *X (Xc)*. The slope of the linear regression line was found to be 0.9964 indicating that the calibrated values of X are almost equal to the known values of X. Similarly, Figure 21 shows the graph between the *Known Y* vs. calibrated value of *Y (Yc)*. The slope of the linear regression line was found to be 1.0109 indicating that the calibrated values of Y are very close to the known values of Y.

The average percentage error between the known and calibrated values of X coordinate of COP was found to be 3.3±2.8%. Similarly, the average percentage error between the known and calibrated values of Y coordinate of COP was found to be 3.2±3.5%.

<center>Representative Plot</center>

A patient with 11.8 cm SVA was compared to an age (66 years v 62 years) and BMI (36.3 kg/m^2 v 32.4 kg/m^2) matched control. In Figure 22, COP displacements in

medio-lateral and anterior-posterior directions are plotted. The graph shows many fold higher path length (1290.7 mm v 221.2 mm), sway area (1179.8 mm^2 v 91.7 mm^2), RMS sway velocity (medio-lateral) (0.07 v 0.38 mm/sec), RMS sway velocity (anterior-posterior) (0.11 v 0.82 mm/sec) in the patient. Note the different locations of the two COP plots. There was an anterior shift of the COP plot for the patient as compared to control.

<u>Comparison of Path Length among Patients and Controls</u>

One-way analysis of variance (ANOVA) was performed to study differences in path length among the controls and the four patient groups, i.e. Low SVA-Low PT, Low SVA- High PT, High SVA- Low PT and High SVA- High PT. The assumption of homogeneity of variance have been violated, therefore Welch F-ratio is reported. There was a statistically significant difference between groups as determined by one-way ANOVA (F (4, 50.65) = 6.85, p = .000). A Games-Howell post-hoc test revealed that the path length in High SVA- High PT group (M= 54.0337 cm, SD= 25.52776 cm) was statistically significantly higher than the Low SVA- High PT (M= 37.9065 cm, SD= 18.20048 cm, p = .045), Low SVA-Low PT (M= 32.7093 cm, SD= 14.82284 cm, p = .003) and Control group (M= 31.8543 cm, SD= 8.57811 cm, p= .000). However, there were no statistically significant differences between the other groups. Figure 23 shows the graph comparing the path length among the various patient groups and the controls. Significant differences are also indicated on the graph.

<u>Comparison of Velocity among Patients and Controls</u>

One-way analysis of variance (ANOVA) was performed to study differences in RMS Sway Velocity in medio-lateral (X) among the controls and the four patient groups,

i.e. Low SVA-Low PT, Low SVA- High PT, High SVA- Low PT and High SVA- High PT. The assumption of homogeneity of variance have been violated, therefore Welch F-ratio is reported. There was a statistically significant difference between groups as determined by one-way ANOVA (F $(4, 50.944)$ = 5.851, p = .001). A Games-Howell post-hoc test revealed that the RMS velocity-X in High SVA- High PT group (M= .01858159 cm/sec, SD= .009245570 cm/sec) was statistically significantly higher than the Control group (M= .01137893 cm/sec, SD= .003386098 cm/sec, p= .001). However, there were no statistically significant differences between the other groups.

One-way analysis of variance (ANOVA) was performed to study differences in RMS Sway Velocity in anterior- posterior (Y) among the controls and the four patient groups, i.e. Low SVA-Low PT, Low SVA- High PT, High SVA- Low PT and High SVA- High PT. The assumption of homogeneity of variance have been violated, therefore Welch F-ratio is reported. There was a statistically significant difference between groups as determined by one-way ANOVA (F $(4, 51.617)$ = 5.782, p = .001).). A Games-Howell post-hoc test revealed that the sway velocity- Y in High SVA- High PT group (M= .03169940 cm/sec, SD= .017083696 cm/sec) was statistically significantly higher than the Low SVA- High PT (M= .02097400 cm/sec, SD= .012310625 cm/sec, p = .049), Low SVA-Low PT (M= .01755366 cm/sec, SD= .011639773 cm/sec, p = .008) and Control group (M= .01763796 cm/sec, SD= .007158312 cm/sec, p= .001). However, there were no statistically significant differences between the other groups.

One-way analysis of variance (ANOVA) was performed to study differences in RMS Sway Velocity (Total) among the controls and the four patient groups, i.e. Low SVA-Low PT, Low SVA- High PT, High SVA- Low PT and High SVA- High PT. The

assumption of homogeneity of variance have been violated, therefore Welch F-ratio is reported. There was a statistically significant difference between groups as determined by one-way ANOVA (F $(4, 50.537)$ = 6.642, p = .000). A Games-Howell post-hoc test revealed that the sway velocity- total in High SVA- High PT group (M= .03728512cm/sec, SD= .018332117 cm/sec) was statistically significantly higher than the Low SVA- High PT (M= .02545151 cm/sec, SD= .013542178 cm/sec, p = .043), Low SVA-Low PT (M= .02168139 cm/sec, SD= .013122989 cm/sec, p = .008) and Control group (M= .02134497 cm/sec, SD= .006867213 cm/sec, p= .000). However, there were no statistically significant differences between the other groups. Figure 24 compares the sway velocities among the various patient groups and the controls. RMS velocity in medio-lateral direction, RMS velocity in anterior-posterior direction and RMS total velocity are plotted and significant differences are marked on the graph.
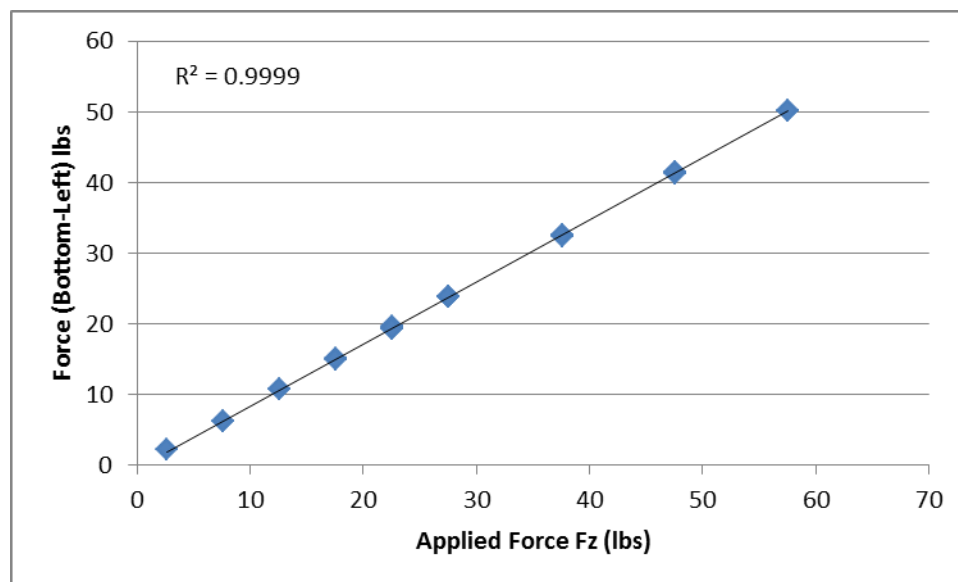
Figure 13. Correlation between the bottom-left sensor force with applied force

Figure 14. Correlation between the bottom-right sensor force with applied force
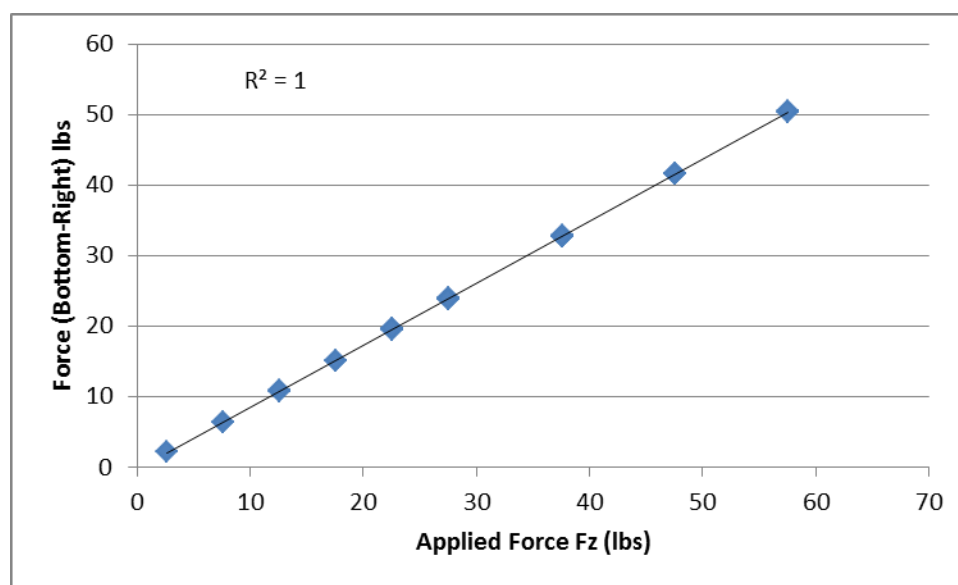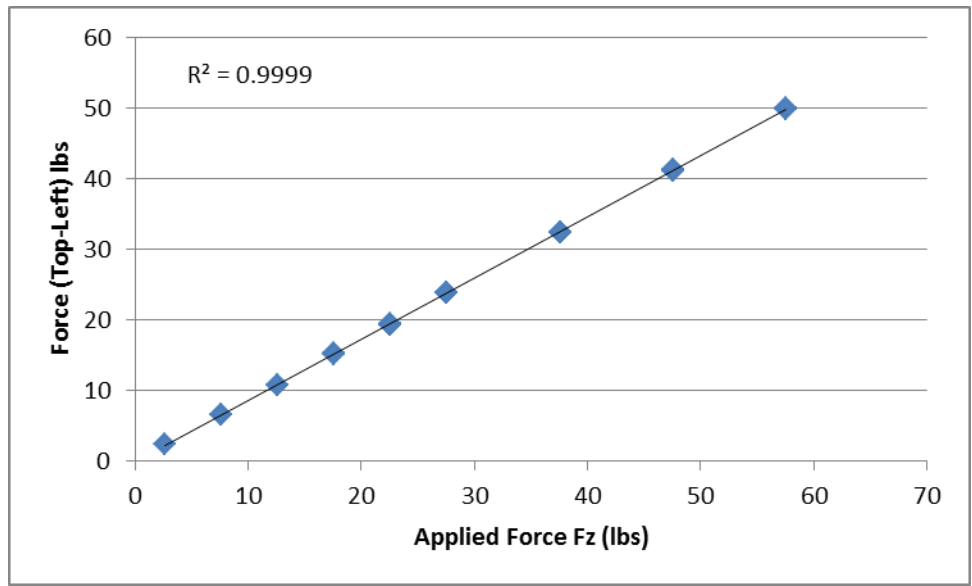
Figure 15. Correlation between the top- left sensor force with applied force
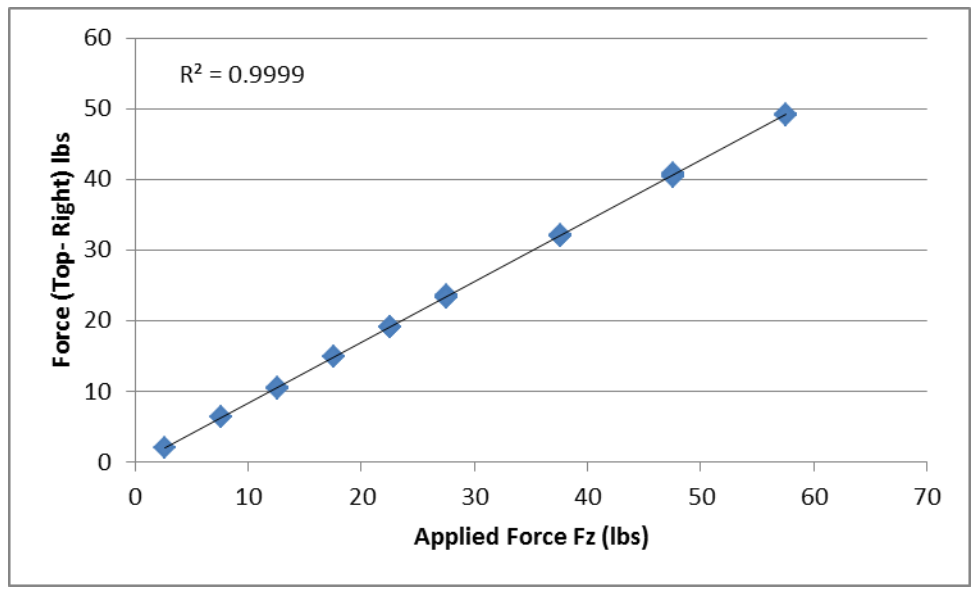
Figure 16. Correlation between the top- right sensor force with applied load
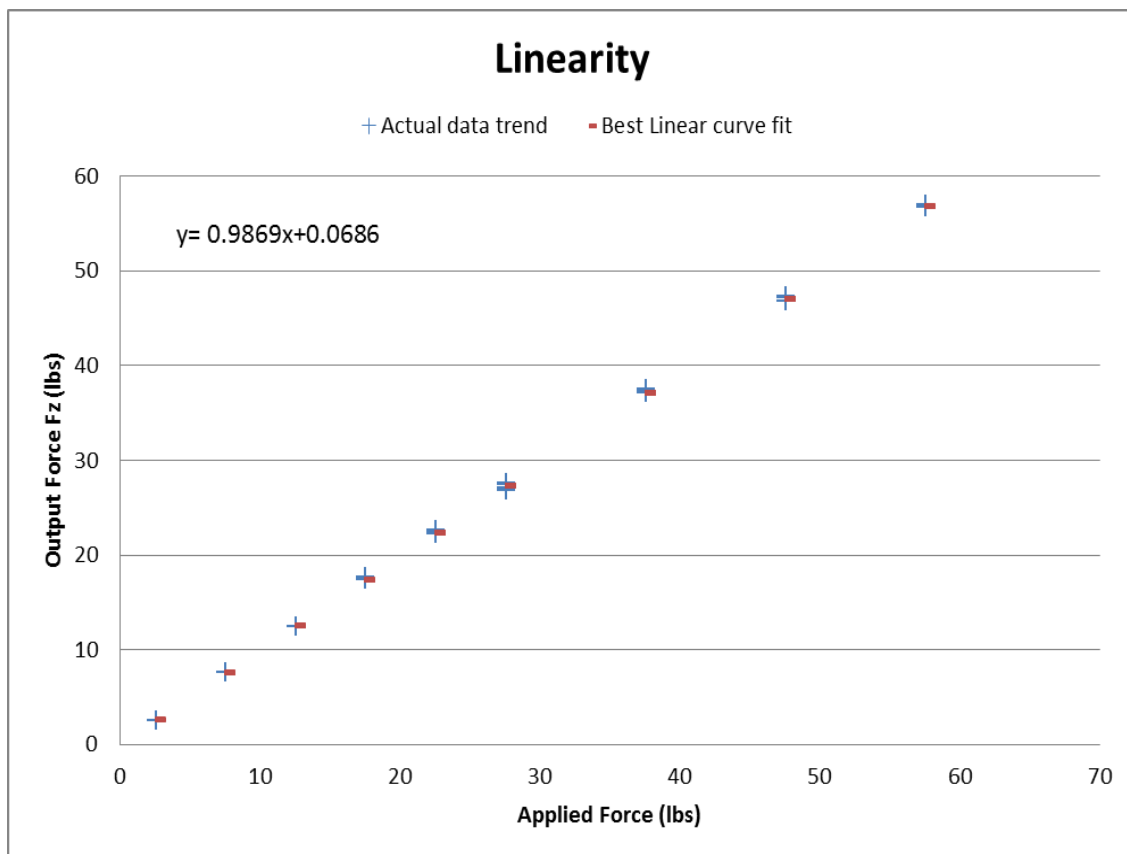
Figure 17. Linearity error for one full cycle of loading
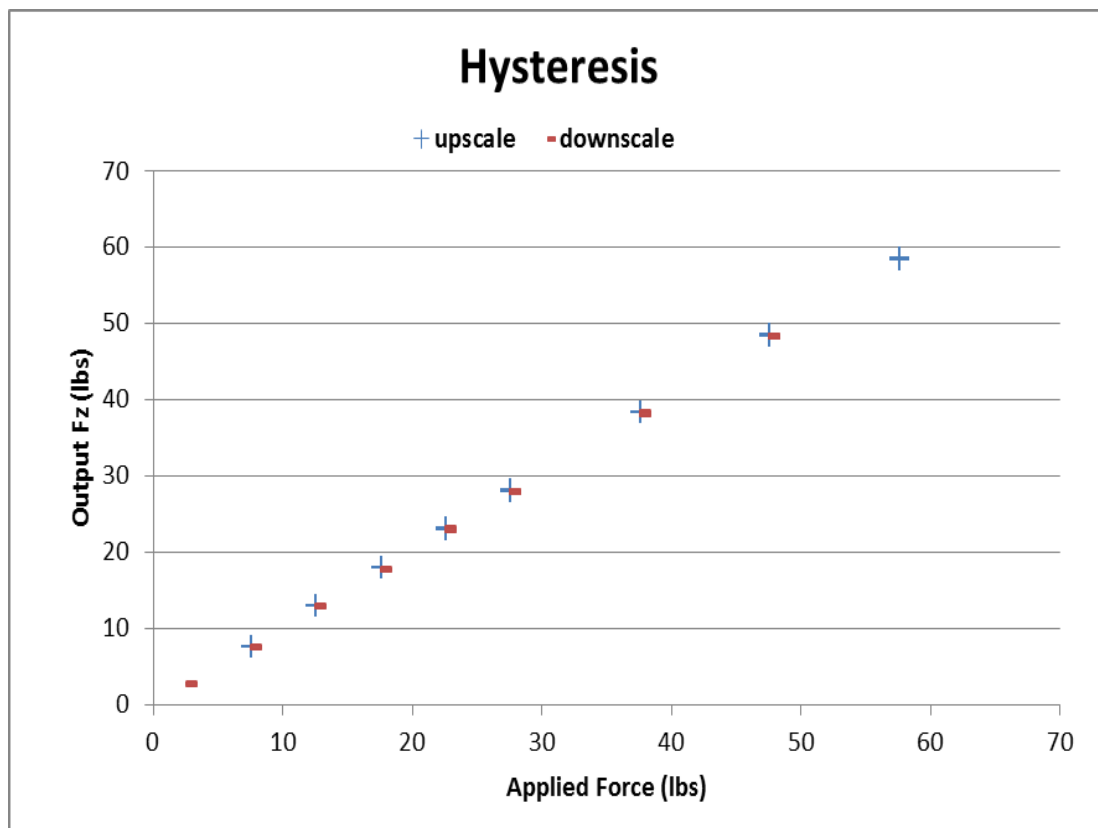
Figure 18. Hysteresis curve for one full cycle of loading and unloading
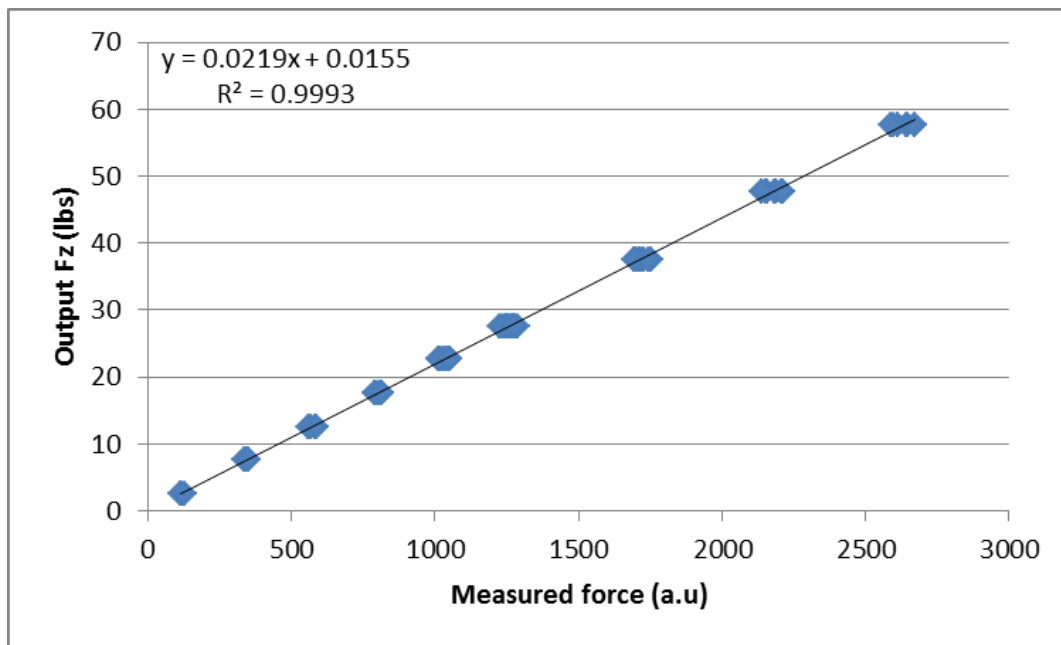
Figure 19. Graph representing measured force (a.u.) vs. output force (lbs)

Known X vs. Xc

$y = 0.9964x - 0.0195$
$R^2 = 0.9992$

Y-axis: Calibrated X (Xc) cm
X-axis: Known X (cm)
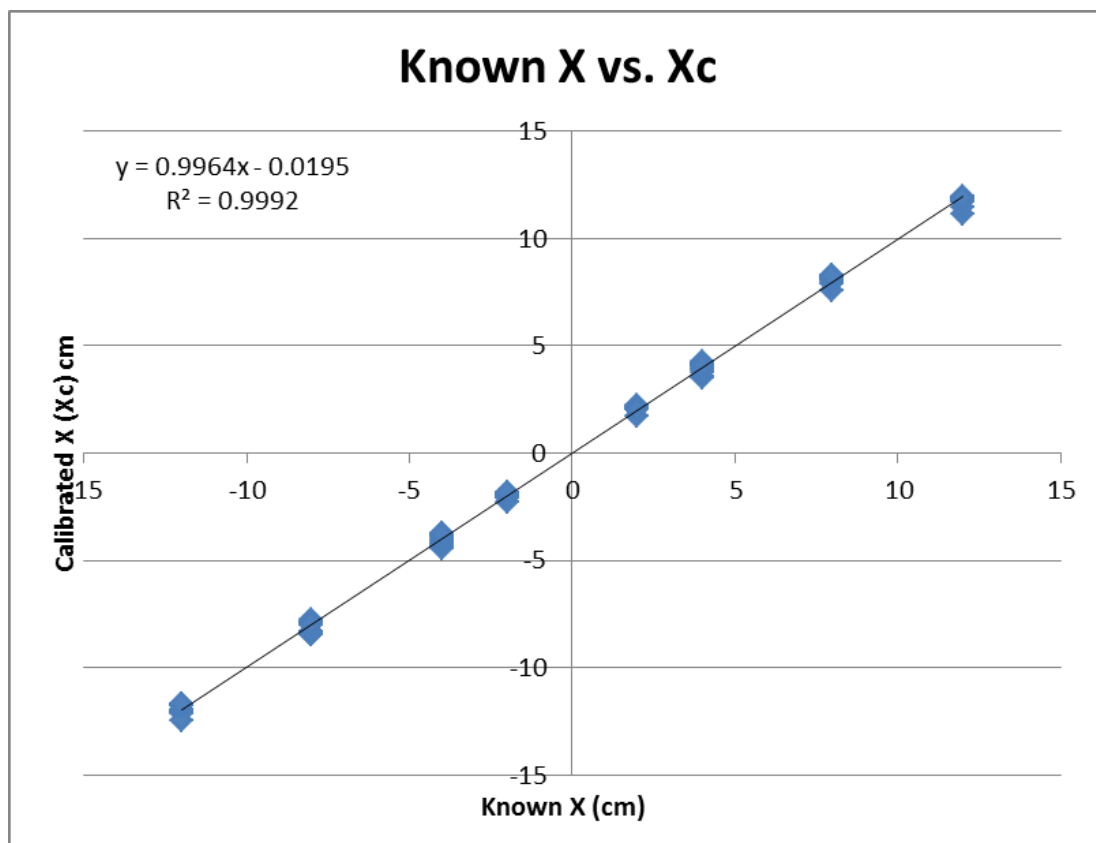
Figure 20. Graph between the Known *X vs.* the calibrated value of *X (Xc)*

Figure 21. Graph between the Known *Y vs.* the calibrated value of *Y(Yc)*
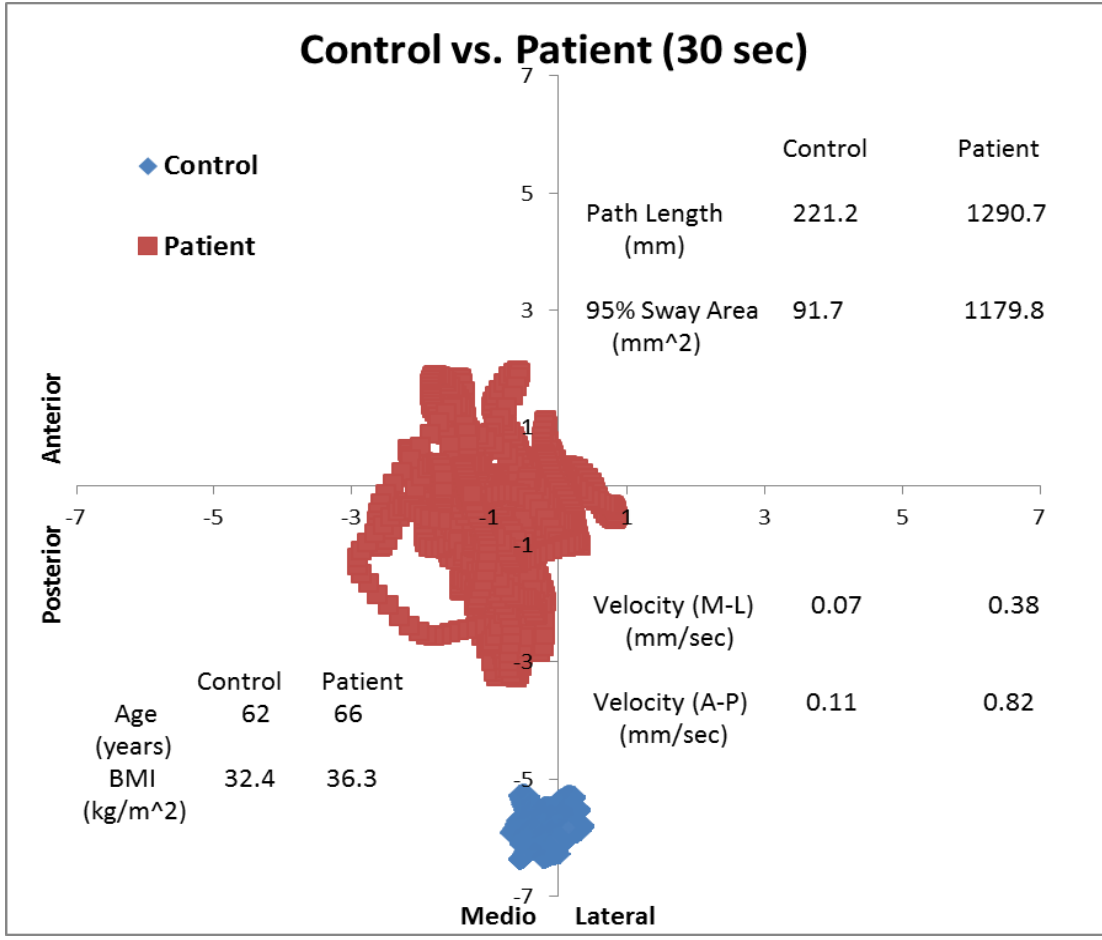
Figure 22. Representative graph between a control and a patient
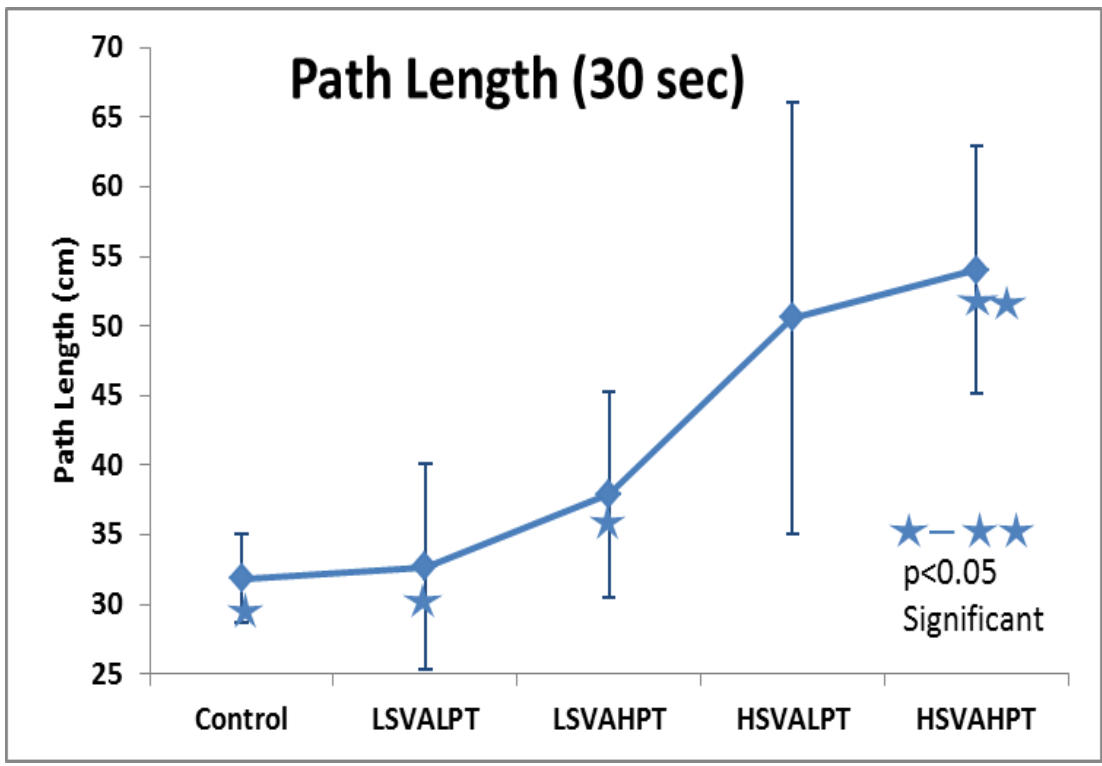
Figure 23. Graph comparing path length between control and patient groups
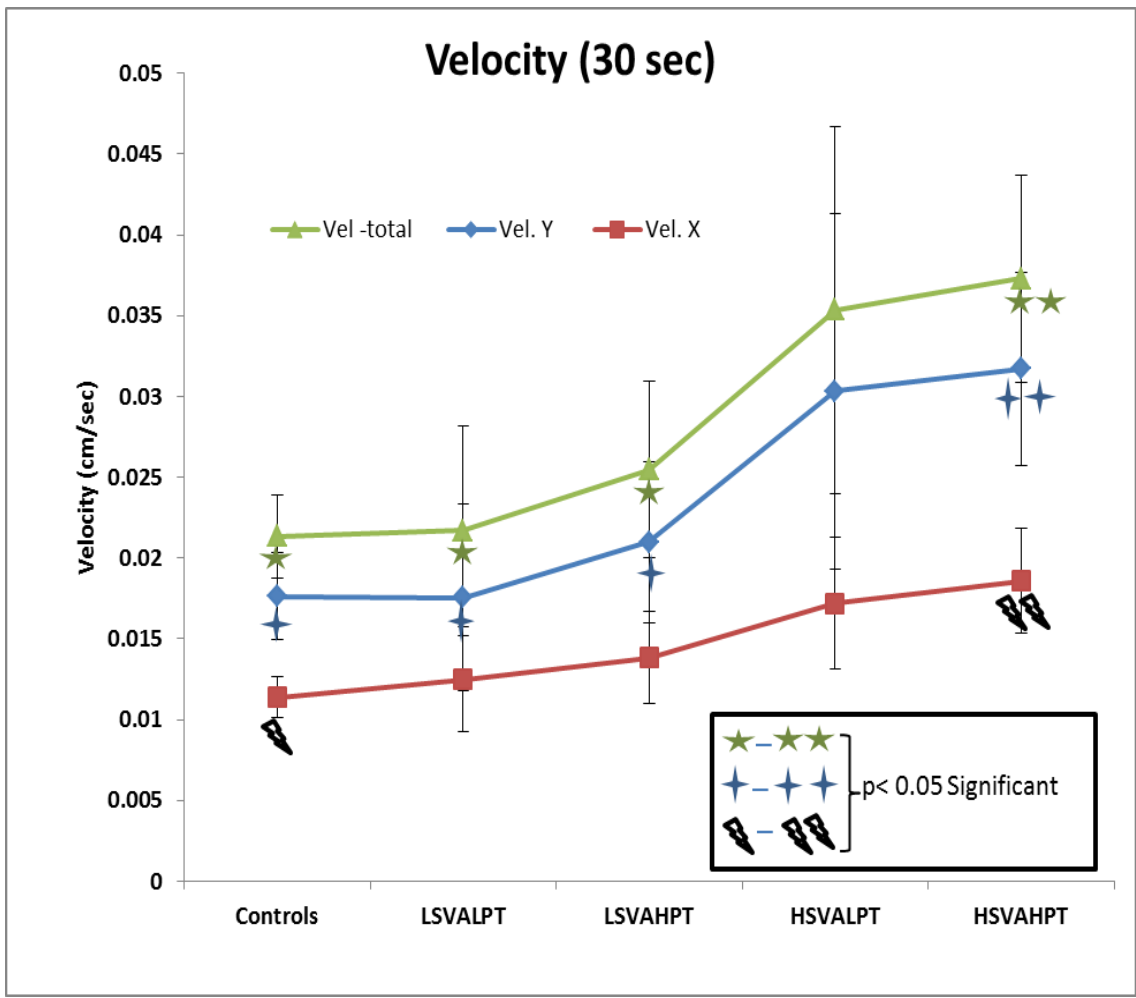
Figure 24. Graph comparing sway velocity between control and patient groups

CHAPTER 5: DISCUSSION

The purpose of the project was to develop a prototype novel balance assessment tool using a WBB. Motivation of the project was to bring the benefits of force plate based assessment of balance such as accuracy, reliability and information about clinically relevant parameters of postural instability into an easy to use, widely available, portable and affordable package. This tool is economic in terms of cost, labor and instrumentation; and can be used in conjunction with functional balance tests to provide more comprehensive information about an individual's postural stability. The outcomes of this project can bring the essence of sophisticated, expensive force plate technology available only in specialized laboratories within the reach of practicing clinicians and therapists.
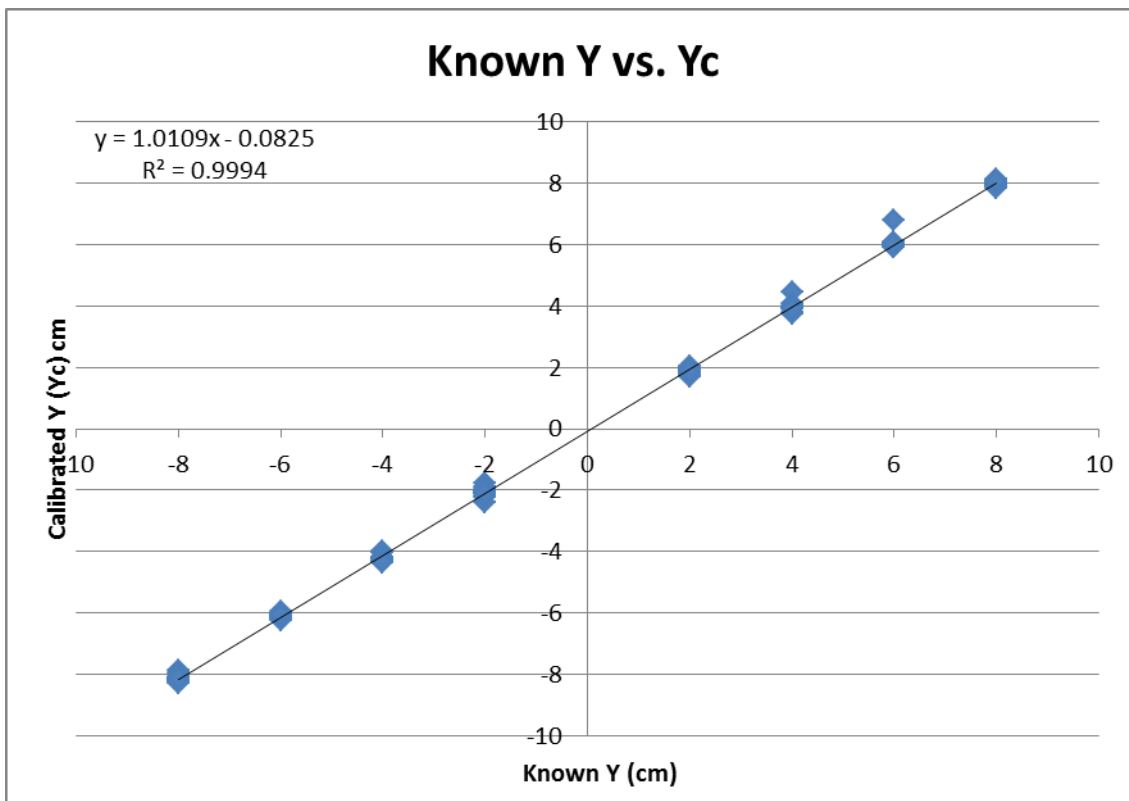
The WBB is a commercially available, rather inexpensive accessory that comes with Wii video games console, has pressure sensors that can be used to determine COP. Exploiting these features into creating a clinical tool for balance studies and fall risk estimation will enhance understanding of balance impairment on patient level. Thus, empowering clinicians/therapists in various fields of rehabilitation, sports medicine, geriatrics, orthopedics, obesity, neurology etc. to study minor damages or changes in postural control and stability, making patient specific recommendations, and prescribing interventions for fall prevention and reducing fall related injuries/ deaths and overall cost spent on it each year.

Linearity of a measurement device is crucial in evaluation of its performance. Non- linearity in a system can be caused by noise, crosstalk etc. Error in a system due to presence of non-linearity is desired to be minimal. It is often studied using percent full

scale output. The non- linearity error of a WBB as studied in this project was found to be higher as compared to Kistler force plate(<1.75 %FSO vs. <0.2 %FSO). (Type 9286B Kistler force plate is designed specifically for use in balance and gait analysis and offers excellent accuracy of COP).

Hysteresis error is the difference in the output of the system between an upscale loading vs. a downscale sequential unloading. It may be caused by the residual charges in the electrical parts. Hysteresis error for a measurement system is defined in terms of %FSO. On comparing the %FSO hysteresis error between WBB and the Kistler force plate, the error in WBB is found higher (<1% FSO vs. <0.3 %FSO).

Although the error due to non- linearity and hysteresis are higher in WBB, it compares well in consideration to the cost (~$5000- 10000 force plates vs. ~$100 WBB) and other factors such as bulky instrumentation, complexity of operation, portability and availability.

<u>Clinical Testing and Validation</u>

Representative Plot

The COP displacements in the medio-lateral and anterior-posterior directions during a 30 second standing trial, comparing a spinal deformity patient with SVA= 11.8 cm and a control reveal that there is an increase in postural sway parameters and instability in the patient. Age and BMI were matched in order to eliminate any significant effects of aging and difference in BMIs on the balance.

Maintenance of upright standing posture and balance depends upon optimal alignment of the spine and pelvis, which keeps the gravity line well within the perimeter of the feet and establishes a posture that is economic in terms of musculoskeletal loads and energy expenditure. Sagittal plane deformities as found in the patient population alter the congruency between spino-pelvic segments, shifting the C7 plumb line and center of gravity towards the periphery of 'cone of balance'. These changes challenge the balance system of the body.

Although compensatory mechanisms are utilized to bring the gravity line within normal ranges, maintenance of these postures is highly uneconomic and result in increased muscular demands thereby fatiguing the supporting muscles and enhance pain. Studies have shown that spinal loads are greatly affected by body posture and 20 degree flexion may result in load of 250% body weight in L3 level, however, there is only 60% of body weight above that level[45].

<div align="center">Comparison of Sway Parameters in Patient Groups and Control</div>

One way ANOVA comparing the means of path length and sway velocity in the three patient groups indicate that the High SVA- High PT group has statistically significant increase in postural instability relative to Low SVA- High PT, Low SVA- Low PT groups and controls. Although, these is a steady increase in the sway parameters in patient groups and controls group, there weren't any significant differences between Low SVA-Low PT, Low SVA- High PT, and High SVA- Low PT groups.

Traditionally, sagittal plane profile is classified into balanced, balanced with compensation and imbalanced groups. The Low SVA- Low PT group is considered to be balanced. The Low SVA- High PT group is marked by the presence of compensatory

mechanisms but balanced. However, the High SVA- Low PT indicate that although imbalance is present, the Pelvic retroversion isn't activated to correct it and High SVA- High PT show presence of compensation up until the point where compensatory changes can no longer restore the gravity line in physiologic range and neutralize positive SVA. At spinal level, reduction of thoracic kyphosis, hyperextension etc. presents them to compensate for anterior translation of gravity line. Pelvic retroversion is usually the first mechanism to set in to correct imbalance, however with progressive deformity it is limited by the parameter of pelvic tilt and hip extension before other mechanisms such as knee flexion and ankle extension are activated.

The degree of presence of these compensatory mechanisms is depended upon a lot of factors such as, severity of deformity, flexibility and stiffness of spine and muscle strength. A combination of these may be activated in varying degree to balance the spine. In addition to above mentioned, factors such as body habitus, exercise capacity, BMI etc. affects the ability of patients to maintain a stable posture.

Nevertheless, there is a steep increase in the sway parameters and postural instability in group with High SVA, with or without High PT.

Another note-worthy observation while comparing velocity in X and Y and total velocity is that the velocity in medio-lateral direction doesn't significantly vary among the patient groups and controls. The major component contributing to significant differences in total velocity is due to changes in velocity in anterior-posterior direction.

This suggests that majority of the total instability is found in anterior posterior direction and that even the patient population is able to control sway and is steadier in the medio-lateral direction.

Significance of Studying Balance in Spinal Deformities

Traditionally, in spinal deformity population, center of balance is studied using radiography. Radiography in assessing spinal balance relies primarily on SVA, i.e. horizontal offset between C7 plumb-line and sacral endplate. However, the effect of compensatory mechanisms decrease positive sagittal imbalance and thus undermine the severity of deformity. Various studies have documented effect of arm position on SVA. In addition to that, radiography provides information about balance in only a single frame of time, doesn't provide knowledge about force distribution and foot position (knee flexion and ankle extension) and has considerable inter-observer and intra-observer variance.

Study of global balance is important because of number of reasons. Spine is a major structure that enables the body to maintain an upright posture and stand with a horizontal gaze. It supports and transfers mechanical loads from the upper body to pelvis and lower extremities. Congruence between spine and pelvis is required to maintain COP of the body within the 'cone of balance' with minimum energy expenditure. Lafage V. et al concluded that even with varying SVA and trunk inclination, pelvic retroversion is employed to maintain the gravity line (COP)- heel position[46].

Limitations and Future work

Limitations of WBB

Circuitry of commercially available WBB is set at sampling rate of 60 Hz, although it may vary and is not always constant. This may be due to quality of sensors, Bluetooth connectivity etc. One of the major limitations of using a WBB is that the

maximum weight that can be detected ~ 330lbs. This can be particularly limiting, in cases of study of balance in obese population.

<div align="center">Validity of the Sway Parameters</div>

One way ANOVA comparing the mean 95% sway area in the three patient groups didn't show any statistically significant differences. It is less sensitive parameter in quantifying and detecting changes in instability and balance. The interpretations made from this parameter may not be entirely valid.

95% sway area is based on a statistical measure that uses standard deviation and covariance in X and Y coordinates, to calculate 95 % confidence region (ellipse) around the mean values of X and Y. Although it's used often in understanding balance, the measure by definition, doesn't include all the displacements registered by the COP signal during a trial. Another reason for its poor sensitivity may be that, especially in patient population the COP displacements seldom follow an elliptical trajectory.

Path length and sway velocity act as relatively valid measures of balance; the measures tracks whole range of COP movement. These are widely used in balance studies and have direct association with instability. COP signal is generated in response to translation in the COG; hence, displacement in the COP signal may also be generated as a result of finer adjustments in the control of COG within the stability limits. The parameter, path length, however, is not discriminating between minor adjustments and larger excursions outside the stable region.

Total sway area would be a suitable parameter that can distinguish between the two cases. The future work would include defining a way to calculate and interpret total sway area.

APPENDIX A: ACRONYMS

1. COP- Center of pressure

2. WBB- Wii balance board

3. GUI- Graphical user interface

4. SVA- Sagittal vertical alignment

5. PT- Pelvic tilt

6. COG- Center of gravity

7. RMS- Root mean square

8. %FSO- Percentage full scale output

9. LSVALPT- Low SVA, Low PT

10. LSVAHPT- Low SVA, High PT

11. HSVALPT- High SVA, Low PT

12. HSVAHPT- High SVA, High PT

APPENDIX B: MATLAB CODE

```matlab
% reads the excel file
num= xlsread('P30.xlsx');

% read X and Y
X1= xlsread('P30.xlsx', 'A1:A1620');
Y1= xlsread('P30.xlsx', 'B1:B1620');

%% Calibration
X1c= (X1*(0.022022345)*(21.48547))/(wt);
Y1c= (Y1*(0.022022345)*(12.21421))/(wt);

% fast fourier transform
X1f= fft(X1c,1620);
Y1f= fft(Y1c,1620);

% Power spectral density
PX1f= (X1f.*conj(X1f))/1620;
PY1f= (Y1f.*conj(Y1f))/1620;


f= 1000/1350*(0:675);
plot(f,PX1f(1:676));

% create 8th order low pass butterworth filter

%normalized cut-off freq= Fc/(fs/2), nfc= 5/(54/2)

[z1,p1]=butter(8,0.185);

% implement filter X
fX1=filtfilt(z1,p1,X1c);

%plot(X1s);

%hold on
%figure;
%plot(fX1);

% implement filter Y
fY1=filtfilt(z2,p2,Y1c);

%hold on %figure;
%plot(fY1s);
%grid on;

%pad the input sequences with zeros
fX1p= padarray(fX1,[54 0], 0);

fY1p= padarray(fY1,[54 0], 0);

%Downsampling
%resample at 45 hz
```

```matlab
fX1ps= resample(fX1p,5,6);
fY1ps= resample(fY1p,5,6);

% Remove padded zeros from the output signal

fX1s= fX1ps(55:1386);
fY1s= fY1ps(55:1386);

%% Check code
% subplot(3,1,1)
% plot(X1);figure(gcf)
% subplot(3,1,2)
% plot(fX1, 'r')
% subplot(3,1,3)
% plot(fX1s, 'g')
% figure;
% subplot(3,1,1)
% plot(Y1);figure(gcf)
% subplot(3,1,2)
% plot(fY1, 'r')
% subplot(3,1,3)
% plot(fY1s, 'g')
% figure;


%% path length 30 sec standing
for i= 1:1331
Pl1(i)= sqrt((fY1s(i+1)-fY1s(i))^2+(fX1s(i+1)-fX1s(i))^2);
end
Pls30sec= sum(Pl1);

%% 95 % Confidence ellipse area

% covariance and variances X and Y
X1m= mean(fX1s);
Y1m= mean(fY1s);

X1std= std(fX1s);
Y1std= std(fY1s);

nfX1s=fX1s-X1m;
nfY1s=fY1s-Y1m;

sX1Y1= (sum(nfX1s.*nfY1s))/(length(nfX1s.*nfY1s));

% Area
SAs30sec= (6*3.14)*sqrt(((X1std^2).*(Y1std^2))-(sX1Y1^2));
C1= cov(fX1s,fY1s);

%% Xrms, Yrms, pathlengthx, pathlengthy,mean velx, mean vely, rms velx,
rms vely

% Xrms
Xrmss30sec=(sqrt(sum(nfX1s.^2)))/length(nfX1s);
```

```
% Yrms
Yrmss30sec=(sqrt(sum(nfY1s.^2)))/length(nfY1s);

% pathlengthx
for i= 1:1331
Plx1(i)= abs(fX1s(i+1)-fX1s(i));
end
Plxs30sec= sum(Plx1);

% pathlengthy
for i= 1:1331
Ply1(i)= abs(fY1s(i+1)-fY1s(i));
end
Plys30sec= sum(Ply1);

% instantaneous velx
vxs30sec= Plx1/0.023;

% instantaneous vely
vys30sec= Ply1/0.023;

% mean velx
mvxs30sec= sum(vxs30sec)/length(vxs30sec);

% mean vely
mvys30sec= sum(vys30sec)/length(vys30sec);

% rms velx
rmsvxs30sec= (sqrt(sum((vxs30sec-mvxs30sec).^2)))/length(vxs30sec);

% rms vely
rmsvys30sec= (sqrt(sum((vys30sec-mvys30sec).^2)))/length(vys30sec);
```

REFERENCES

1. A. B. C. (Anatomy, Biomechanics, Control) of Balance during Standing and Walking. Winter, David A. 1995 ISBN : 0-9699420-0-1.

2. Centers for Disease Control and Prevention, National Center for Injury Prevention and Control. http://www.cdc.gov/homeandrecreationalsafety/falls/fallcost.html.

3. José Ailton O. Carneiro, Taiza E.G. Santos-Pontelli and Eduardo Ferriolli. Obese elderly women exhibit low postural stability: a novel three-dimensional evaluation system. CLINICS 2012;67(5):475-481.

4. Frzovic D, Morris ME, Vowels L. Clinical tests of standing balance: performance of persons with multiple sclerosis. Arch Phys Med Rehabil. 2000 Feb;81(2):215-21.

5. Canbek J, Fulk G, Nof L, Echternach J. Test-retest reliability and construct validity of the tinetti performance-oriented mobility assessment in people with stroke. J Neurol Phys Ther. 2013 Mar;37(1):14-9.

6. C. Sackley, P. Richardson, K. McDonnell, S. Ratib, M. Dewey, H.J. Hill. The reliability of balance, mobility and self-care measures in a population of adults with a learning disability known to a physiotherapy service. Clinical Rehabilitation, 19 (2) (2005), pp. 216–223.

7. Schülein S. Comparison of the performance-oriented mobility assessment and the Berg balance scale : Assessment tools in geriatrics and geriatric rehabilitation. Z Gerontol Geriatr. 2013 Apr 27. [Epub ahead of print].

8. Muir SW, Berg K, Chesworth B, Klar N, Speechley M. Quantifying the magnitude of risk for balance impairment on falls in community-dwelling older adults: a systematic review and meta-analysis. J Clin Epidemiol. 2010 Apr;63(4):389-406.

9. R.A. Clark, A.L. Bryant, Y. Pua, P. McCrory, K. Bennell, M. Hunt. Validity and reliability of the Nintendo Wii Balance Board for assessment of standing balance. Gait & Posture, 31 (2010), pp. 307–310.

10. Huurnink A, Fransz DP, Kingma I, van Dieën JH. Comparison of a laboratory grade force platform with a Nintendo Wii Balance Board on measurement of postural control in single-leg stance balance tasks. J Biomech. 2013 Mar 22. pii: S0021-9290(13)00098-5.

11. Aebi M. The adult scoliosis. Eur Spine J. 2005 Dec;14(10):925-48. Epub 2005 Nov 18.

12. Barrey C, Roussouly P, Perrin G, Le Huec JC. Sagittal balance disorders in severe degenerative spine. Can we identify the compensatory mechanisms? Eur Spine J. 2011 Sep;20 Suppl 5:626-33.

13. Dubousset J: Three-dimensional analysis of the scoliotic deformity, in Weinstein SL

(ed): The Pediatric Spine: Principles and Practice. New York, NY: Raven Press, 1994, pp 479-496.

14. Glassman SD, Berven S, Bridwell K, Horton W, Dimar JR.Correlation of radiographic parameters and clinical symptoms in adult scoliosis. Spine (Phila Pa 1976). 2005 Mar 15;30(6):682-8.

15. Glassman SD, Bridwell K, Dimar JR, Horton W, Berven S, Schwab F. The impact of positive sagittal balance in adult spinal deformity. Spine (Phila Pa 1976). 2005 Sep 15;30(18):2024-9.

16. Schroeder J, Schaar H, Mattes K. Spinal alignment in low back pain patients and age-related side effects: a multivariate cross-sectional analysis of video rasterstereography back shape reconstruction data. Eur Spine J. 2013 Apr 25. [Epub ahead of print].

17. Willigenburg NW, Kingma I, van Dieën JH. Center of pressure trajectories, trunk kinematics and trunk muscle activation during unstable sitting in low back pain patients. Gait Posture. 2013 Mar 5. pii: S0966-6362(13)00123-9. gaitpost.2013.02.010. [Epub ahead of print].

18. Ruhe A, Fejer R, Walker B. Pain relief is associated with decreasing postural sway in patients with non-specific low back pain. BMC Musculoskelet Disord. 2012 Mar 21;13:39.

19. Brumagne S; Janssens L; Knapen S; Claeys K: Suuden-Johanson E: Persons with Recurrent Low Back Pain Exhibit a Rigid Postural Control Strategy. Eur. Spine J. 2008 Sep; 17(9): 1177-84.

20. Centers for Disease Control and Prevention, National Center for Injury Prevention and Control. http://www.cdc.gov/homeandrecreationalsafety/falls/fallcost.html.

21. Ogden CL, Carroll MD, Kit BK and Flegal KM. Prevalence of Obesity in the United States, 2009–2010 2012. NCHS Data Brief No. 82.

22. Ku PX, Abu Osman NA, Yusof A, Wan Abas WA. Biomechanical evaluation of the relationship between postural control and body mass index. J Biomech. 2012 Jun 1;45(9):1638-42.

23. Dutil M, Handrigan GA, Corbeil P, Cantin V, Simoneau M, Teasdale N, Hue O. The impact of obesity on balance control in community-dwelling older women. Age (Dordr). 2013 Jun;35(3):883-90.

24. Kasukawa Y, Miyakoshi N, Hongo M, Ishikawa Y, Noguchi H, Kamo K, Sasaki H, Murata K, Shimada Y. Relationships between falls, spinal curvature, spinal mobility and back extensor strength in elderly people. J Bone Miner Metab. 2010;28(1):82-7.

25. Lucy S.D, Hayes K.C. Postural sway profiles, normal subjects and subjects with cerebellar ataxia. Physio. 1985; 37:140-148.

26. Joseph, S. A., Moreno, A. P., Brandoff, J., Casden, A. C., Kuflik, P., & Neuwirth, M. G. (2009). Sagittal plane deformity in the adult patient. The Journal of the American Academy of Orthopaedic Surgeons, 17(6), 378–388.

27. Boulay C, Tardieu C, Hecquet J, et al: Sagittal alignment of spine and pelvis regulated by pelvic incidence: Standard values and prediction of lordosis. Eur Spine J 2006;15:415-422.

28. Roussouly, P., Gollogly, S., Noseda, O., Berthonnaud, E., & Dimnet, J. (2006). The vertical projection of the sum of the ground reactive forces of a standing patient is not the same as the C7 plumb line: a radiographic study of the sagittal alignment of 153 asymptomatic volunteers. Spine, 31(11), E320–5.

29. Mac-Thiong, J.-M., Transfeldt, E. E., Mehbod, A. A., Perra, J. H., Denis, F., Garvey, T. A., Lonstein, J. E., et al. (2009). Can c7 plumbline and gravity line predict health related quality of life in adult scoliosis? Spine, 34(15), E519–27.

30. Barrey C, Roussouly P, Perrin G, Le Huec JC. Sagittal balance disorders in severe degenerative spine. Can we identify the compensatory mechanisms? Eur Spine J. 2011 Sep;20 Suppl 5:626-33.

31. Le Huec JC, Charosky S, Barrey C, Rigal J, Aunoble S. Sagittal imbalance cascade for simple degenerative spine and consequences: algorithm of decision for appropriate treatment. Eur Spine J. 2011 Sep;20 Suppl 5:699-703.

32. Lafage V, Schwab F, Patel A, Hawkinson N, Farcy JP. Pelvic tilt and truncal inclination: two key radiographic parameters in the setting of adults with spinal deformity. Spine (Phila Pa 1976). 2009 Aug 1;34(17):E599-606.

33. Mendoza-Lattes S, Ries Z, Gao Y, Weinstein SL. Natural history of spinopelvic alignment differs from symptomatic deformity of the spine. Spine (Phila Pa 1976). 2010 Jul 15;35(16):E792-8.

34. Marks M, Stanford C, Mahar A, Newton P. Standing lateral radiographic positioning does not represent customary standing balance. Spine (Phila Pa 1976). 2003 Jun 1;28(11):1176-82.

35. Marks M, Stanford C, Newton P. Which lateral radiographic positioning technique provides the most reliable and functional representation of a patient's sagittal balance? Spine (Phila Pa 1976). 2009 Apr 20;34(9):949-54.

36. Faro FD, Marks MC, Pawelek J, Newton PO. Evaluation of a functional position for lateral radiograph acquisition in adolescent idiopathic scoliosis. Spine (Phila Pa 1976). 2004 Oct 15;29(20):2284-9.

37. Aota Y, Saito T, Uesugi M, Ishida K, Shinoda K, Mizuma K. Does the fists-on-clavicles position represent a functional standing position? Spine (Phila Pa 1976). 2009 Apr 15;34(8):808-12. doi: 10.1097/BRS.0b013e31819e2191.

38. Roussouly P, Gollogly S, Noseda O, Berthonnaud E, Dimnet J. The vertical projection of the sum of the ground reactive forces of a standing patient is not the same as the C7 plumb line: a radiographic study of the sagittal alignment of 153 asymptomatic volunteers. Spine (Phila Pa 1976). 2006 May 15;31(11):E320-5.

39. Zaina F, Pizzetti P, Donzelli S, Negrini F, Negrini S. Why X-rays are not reliable to assess sagittal profile: a cross sectional study. Stud Health Technol Inform. 2012;176:268-72.

40. National Instruments forums. http://forums.ni.com/t5/LabVIEW/Use-Wii-Balance-Board-in-LabVIEW/td-p/710740.

41. Bobbert MF, Schamhardt HC. Accuracy of determining the point of force application with piezoelectric force plates. Journal of Biomechanics 1990; 23(7):705-710.

42. Collins SH, Adamczyk PG, Ferris DP, Kuo AD. A simple method for calibrating force plates and force treadmills using an instrumented pole. Gait Posture. 2009 Jan;29(1):59-64. doi: 10.1016/j.gaitpost.2008.06.010. Epub 2008 Aug 27.

43. Kistler. 1984 Multicomponent measuring force plate for Biomechanics and Industry type 9287, Kistler Switzerland.

44. Stins JF, Ledebt A, Emck C, van Dokkum EH, Beek PJ. Patterns of postural sway in high anxious children. Behav Brain Funct. 2009 Oct 2;5:42. doi: 10.1186/1744-9081-5-42.

45. Nachemson A. The load on lumbar discs in different positions of the body. Clin Orthop Relat Res. 1966 Mar-Apr;45:107-22.

46. Lafage V, Schwab F, Skalli W, Hawkinson N, Gagey PM, Ondra S, Farcy JP. Standing balance and sagittal plane spinal deformity: analysis of spinopelvic and gravity line parameters. Spine (Phila Pa 1976). 2008 Jun 15;33(14):1572-8.